References

[1] Minnikin, D. E. (1982) Presented at the Part I. Physiology of the mycobacteria. In The Biology of the Mycobacteria.

[2] Rastogi, N., Legrand, E. and Sola, C. (2001) The mycobacteria: an introduction to nomenclature and pathogenesis. Rev. Sci. Tech. 20, 21–54.

[3] Ryll, R., Kumazawa, Y. and Yano, I. (2001) Immunological properties of trehalose dimycolate (cord factor) and other mycolic acid-containing glycolipids – a review. Microbiol. Immunol. 45, 801–811.

[4] Fujiwara, N. (1997) Distribution of antigenic glycolipids among *Mycobacterium tuberculosis* strains and their contribution to virulence. Kekkaku 72, 193–205.

[5] Coelho, E.A., Tavares, C.A., de Melo Lima, K., Silva, C.L., Rodrigues Jr., J.M. and Fernandes, A.P. (2006) *Mycobacterium* hsp65 DNA entrapped into TDM-loaded PLGA microspheres induces protection in mice against *Leishmania (Leishmania) major* infection. Parasitol. Res. 98, 568–575.

[6] Oiso, R., Fujiwara, N., Yamagami, H., Maeda, S., Matsumoto, S., Nakamura, S., Oshitani, N., Matsumoto, T., Arakawa, T. and Kobayashi, K. (2005) Mycobacterial trehalose 6,6′-dimycolate preferentially induces type 1 helper T cell responses through signal transducer and activator of transcription 4 protein. Microb. Pathog. 39, 35–43.

[7] Hunter, R.L., Olsen, M.R., Jagannath, C. and Actor, J.K. (2006) Multiple roles of cord factor in the pathogenesis of primary, secondary, and cavitary tuberculosis, including a revised description of the pathology of secondary disease. Ann. Clin. Lab. Sci. 36, 371–386.

[8] Dhariwal, K.R., Yang, Y.-M., Fales, H.M. and Goren, M.B. (1987) Detection of trehalose monomycolate in *Mycobacterium leprae* grown in armadillo tissues. J. Gen. Microbiol. 133, 201–209.

[9] Prome, J.C., Lacave, C.A., Ahibo-Coffy and Savagnac, A. (1976) Separation of structural studies of the molecular species of monomycolates and dimycolates of alpha-D-trehalose present in *Mycobacterium phlei.* Eur. J. Biochem. 63, 543–552.

[10] Wang, L., Izumi, S., He, H., Fujiwara, N., Saita, N., Yano, I., Kobayashi, K. and Tatsumi, N. (1999) Serodiagnosis of Hansen's disease/leprosy by enzyme-linked immunosorbent assay using cord factor (trehalose 6,6′-dimycolate) as an antigen. Nihon Hansenbyo Gakkai Zasshi 68, 165–174.

[11] Goren, M.B., Brokl, O. and Roller, P. (1979) Cord factor (trehalose-6,6′-dimycolate) of in vivo-derived *Mycobacterium lepraemurium.* Biochim. Biophys. Acta 574, 70–78.

[12] Fujita, Y., Ogata, H. and Yano, I. (2005) Clinical evaluation of serodiagnosis of active tuberculosis by multiple-antigen ELISA using lipids from *Mycobacterium bovis* BCG Tokyo 172. Clin. Chem. Lab. Med. 43, 1253–1262.

[13] Sasaki, N., Kawatsu, K., Tsutsumi, S., Gidoh, M., Nakagawa, H., Kashiwabara, Y., Matsuki, G. and Endo, H. (1997) Pathological investigation of armadillos infected with *Mycobacterium leprae.* Nihon Hansenbyo Gakkai Zasshi 66, 227–235.

[14] Fujita, Y., Naka, T., Doi, T. and Yano, I. (2005) Direct molecular mass determination of trehalose monomycolate from 11 species of mycobacteria by MALDI-TOF mass spectrometry. Microbiology 151, 1443–1452.

[15] Fujita, Y., Naka, T., McNeil, M.R. and Yano, I. (2005) Intact molecular characterization of cord factor (trehalose 6,6′-dimycolate) from nine species of mycobacteria by MALDI-TOF mass spectrometry. Microbiology 151, 3403–3416.

[16] Minnikin, D.E. and Polgar, N. (1967) Synthesis of methyl 3,12,15-trimethyldocosanoate and 3,15-dimethyldocosanoate. J. Chem. Soc. 7, 575–577.

[17] Yuan, Y., Crane, D.C., Musser, J.M., Sreevatsan, S. and Barry 3rd., C.E. (1997) MMAS-1, the branch point between *cis-* and *trans-*cyclopropane-containing oxygenated mycolates in *Mycobacterium tuberculosis.* J. Biol. Chem. 272, 10041–10049.

[18] Draper, P., Dobson, G., Minnikin, D.E. and Minnikin, S.M. (1982) The mycolic acids of *Mycobacterium leprae* harvested from experimentally infected nine-banded armadillos. Ann. Microbiol. 133, 39–47.

[19] Takayama, K., Wang, C. and Besra, G.S. (2005) Pathway to synthesis and processing of mycolic acids in *Mycobacterium tuberculosis.* Clin. Microbiol. Rev. 18, 81–101.

[20] Minnikin, D.E., Dobson, G., Goodfellow, M., Draper, P. and Magnusson, M. (1985) Quantitative comparison of the mycolic and fatty acid compositions of *Mycobacterium leprae* and *Mycobacterium gordonae.* J. Gen. Microbiol. 131, 2013–2021.

[21] Watanabe, M., Aoyagi, Y., Mitome, H., Fujita, T., Naoki, H., Ridell, M. and Minnikin, D.E. (2002) Location of functional groups in mycobacterial meromycolate chains; the recognition of new structural principles in mycolic acids. Microbiology 148, 1881–1902.

[22] Watanabe, M., Aoyagi, Y., Ridell, M. and Minnikin, D.E. (2001) Separation and characterization of individual mycolic acids in representative mycobacteria. Microbiology 147, 1825–1837.

[23] Glickman, M.S., Cahill, S.M. and Jacobs Jr., W.R. (2001) The *Mycobacterium tuberculosis* cmaA2 gene encodes a mycolic acid *trans-*cyclopropane synthetase. J. Biol. Chem. 276, 2228–2233.

[24] Yuan, Y., Zhu, Y., Crane, D.D. and Barry 3rd., C.E. (1998) The effect of oxygenated mycolic acid composition on cell wall function and macrophage growth in *Mycobacterium tuberculosis.* Mol. Microbiol. 29, 1449–1458.

[25] Bhatt, A., Fujiwara, N., Bhatt, K., Gurcha, S.S., Kremer, L., Chen, B., Chan, J., Porcelli, S.A., Kobayashi, K., Besra, G.S. and Jacobs Jr., W.R. (2007) Deletion of *kasB* in *Mycobacterium tuberculosis* causes loss of acid-fastness and subclinical latent tuberculosis in immunocompetent mice. Proc. Natl. Acad. Sci. USA 104, 5157–5162.

[26] Hunter, S.W. and Brennan, P.J. (1981) A novel phenolic glycolipid from *Mycobacterium leprae* possibly involved in immunogenicity and pathogenicity. J. Bacteriol. 147, 728–735.

[27] Daffe, M. and Laneelle, M.A. (1989) Diglycosyl phenol phthiocerol diester of *Mycobacterium leprae.* Biochim. Biophys. Acta 1002, 333–337.

Characterization of the Fucosylation Pathway in the Biosynthesis of Glycopeptidolipids from *Mycobacterium avium* Complex[∇]

Yuji Miyamoto,[1] Tetsu Mukai,[1]* Yumi Maeda,[1] Noboru Nakata,[1] Masanori Kai,[1]
Takashi Naka,[2] Ikuya Yano,[2] and Masahiko Makino[1]

Department of Microbiology, Leprosy Research Center, National Institute of Infectious Diseases, 4-2-1 Aobacho, Higashimurayama, Tokyo 189-0002, Japan,[1] and Japan BCG Central Laboratory, 3-1-5 Matsuyama, Kiyose, Tokyo 204-0022, Japan[2]

The cell envelopes of several species of nontuberculous mycobacteria, including the *Mycobacterium avium* complex, contain glycopeptidolipids (GPLs) as major glycolipid components. GPLs are highly antigenic surface molecules, and their variant oligosaccharides define each serotype of the *M. avium* complex. In the oligosaccharide portion of GPLs, the fucose residue is one of the major sugar moieties, but its biosynthesis remains unclear. To elucidate it, we focused on the 5.0-kb chromosomal region of the *M. avium* complex that includes five genes, two of which showed high levels of similarity to the genes involved in fucose synthesis. For the characterization of this region by deletion and expression analyses, we constructed a recombinant *Mycobacterium smegmatis* strain that possesses the *rtfA* gene of the *M. avium* complex to produce serovar 1 GPL. The results revealed that the 5.0-kb chromosomal region is responsible for the addition of the fucose residue to serovar 1 GPL and that the three genes *mdhtA*, *merA*, and *gtfD* are indispensable for the fucosylation. Functional characterization revealed that the *gtfD* gene encodes a glycosyltransferase that transfers a fucose residue via 1→3 linkage to a rhamnose residue of serovar 1 GPL. The other two genes, *mdhtA* and *merA*, contributed to the formation of the fucose residue and were predicted to encode the enzymes responsible for the synthesis of fucose from mannose based on their deduced amino acid sequences. These results indicate that the fucosylation pathway in GPL biosynthesis is controlled by a combination of the *mdhtA*, *merA*, and *gtfD* genes. Our findings may contribute to the clarification of the complex glycosylation pathways involved in forming the oligosaccharide portion of GPLs from the *M. avium* complex, which are structurally distinct.

Mycobacteria have a unique multilayer cell envelope composed of peptidoglycan, arabinogalactan, mycolic acids, and an outer layer that contains abundant species-specific glycolipids. It is thought that these cell wall characteristics allow mycobacteria to survive in host cells (8, 11). Among the glycolipids present in the outer layer of the cell envelope, glycopeptidolipids (GPLs) are recognized as highly antigenic surface molecules in several species of nontuberculous mycobacteria, including the *Mycobacterium avium* complex (29). The common structure in which the fatty acyl-tetrapeptide core is glycosylated with both 6-deoxy-talose (6-d-Tal) and *O*-methyl-rhamnose (*O*-Me-Rha), termed core GPLs, is present in all types of GPLs (2, 4, 12). The core GPLs are further glycosylated with a Rha residue or various oligosaccharides linked to the 6-d-Tal residue. These glycosylation events give rise to structural variations, especially in the GPLs from the *M. avium* complex, that are responsible for the creation of serotypes, and they are also known as serovar-specific GPLs (ssGPLs). The ssGPLs define approximately 30 serotypes, some of which are found predominantly in isolates from patients. For example, the serotypes 1, 4, 6, and 8 are frequently isolated from AIDS patients coinfected with the *M. avium* complex (17, 30). In addition, ssGPLs are associated with host responses to infection and func-

tion as agonists of cell surface receptors such as Toll-like receptor 2 (28).

The biosynthesis of GPLs, including methylation, acetylation, and peptide synthesis, has been investigated mainly with *M. smegmatis*, but it has not been fully elucidated (6, 15, 21, 23). We have recently identified the glycosyltransferase genes involved in the formation of core GPLs in *M. smegmatis* and *M. avium* (19), but the glycosylation pathways of ssGPLs have not been clarified, except for that of serovar 1 GPL (14). The presence of a Rha residue linked to 6-d-Tal, as observed with serovar 1 GPL, is structurally required for the formation of all types of ssGPLs. The Rha residue is further extended by the subsequent addition of one of the three different sugars, Rha, fucose (Fuc), or glucose, to form the structural group of ssGPLs (9). In these groups, the Fuc-containing ssGPLs, such as serovar 2, 3, 4, and 9 GPLs, shown in Table 1, comprise the major group in the ssGPLs of the *M. avium* complex, and serovar 2 GPL is the basic structure for these ssGPLs (9). The biosynthetic pathway for the Fuc-containing ssGPLs is still unclear. In the *M. avium* complex, a 22- to 25-kb chromosomal region with the ability to synthesize the serovar 2 GPL has been identified and cloned from two strains (4, 5). However, the key genes responsible for the formation of the Fuc residue of serovar 2 GPL have not been identified in this chromosomal region. In this study, we have focused on a 5.0-kb segment that includes the genes predicted to be associated with Fuc synthesis and have characterized their functions in the biosynthesis of GPLs in the *M. avium* complex.

---

* Corresponding author. Mailing address: Department of Microbiology, Leprosy Research Center, National Institute of Infectious Diseases, 4-2-1 Aobacho, Higashimurayama, Tokyo 189-0002, Japan. Phone: 81-42-391-8211. Fax: 81-42-394-9092. E-mail: tmukai@nih.go.jp.

TABLE 1. Oligosaccharide structures of Fuc-containing ssGPLs

Serotype	Oligosaccharide[a]
2	2,3-di-O-Me-α-L-Fuc-(1→3)-α-L-Rha-(1→2)-L-6-d-Tal
4	4-O-Me-α-L-Rha-(1→4)-2-O-Me-α-L-Fuc-(1→3)-α-L-Rha-(1→2)-L-6-d-Tal
3	2,3-di-O-Me-α-L-Fuc-(1→4)-β-D-GlcA-(1→4)-2,3-di-O-Me-α-L-Fuc-(1→3)-α-L-Rha-(1→2)-L-6-d-Tal
9	4-O-Ac-2,3-di-O-Me-α-L-Fuc-(1→4)-β-D-GlcA-(1→4)-2,3-di-O-Me-α-L-Fuc-(1→3)-α-L-Rha-(1→2)-L-6-d-Tal

[a] The oligosaccharide structures are from reference 9. GlcA, glucuronic acid; Ac, acetyl.

MATERIALS AND METHODS

Bacterial strains, culture conditions, and DNA manipulation. The bacterial strains and vectors used and constructed in this study are listed in Table 2. *M. avium*, used for the isolation of chromosomal DNA, was grown in Middlebrook 7H9 broth (Difco) with 0.05% Tween 80 supplemented with 10% Middlebrook ADC enrichment broth (BBL). Recombinant *M. smegmatis* strains for GPL production were cultured in Luria-Bertani broth with 0.2% Tween 80. The isolation of DNA, transformation, and PCR were carried out as previously described (20). *Escherichia coli* strain DH5α was used for the routine manipulation and propagation of plasmid DNA. The following antibiotics were added as required: kanamycin, 50 μg/ml for *E. coli* and 25 μg/ml for *M. smegmatis*; hygromycin B, 150 μg/ml for *E. coli* and 75 μg/ml for *M. smegmatis*. Oligonucleotide primers used for PCR are available on request.

Construction of the integrating mycobacterial vector (pYM301). The site-specific integrating mycobacterial vector pYM301 was constructed from parts of pYUB854, pMV306kan, and pMV261 (3, 24, 27). To replace the *oriM* region of pMV261 with the region needed for integration, a fragment containing *attP* and *int* was amplified from pMV306kan DNA using the primers INT-S and INT-A, digested with the respective restriction enzyme, and cloned into the XbaI-MluI site of pMV261 to give pMV301kan. The hygromycin-resistant cassette, a selective marker of integration, was excised from pYUB854 with XbaI and NheI and inserted into the NheI-SpeI site of pMV301kan to obtain *hyg* instead of *kan*. Because the resulting plasmid had restriction sites for EcoRI, BamHI, and PstI outside of the multicloning site, it was disrupted in turn by PCR to create pYM301 by using the following primers: 301ECO-D and 301ECO-U for disruption of the EcoRI site, 301PST-D and 301PST-U for disruption of the PstI site, and 301BAM-D and 301BAM-U for disruption of the BamHI site.

Construction of expression vectors. Previous studies have shown that the clustered *gtfC-gtfD* region is about 5.0 kb long and contains five genes, designated *gtfC, mdhtA, merA, mtfF,* and *gtfD* (13). To express these five genes as one operon, the 5.0-kb segment was obtained as a PstI-EcoRI fragment to be inserted

into the expression cassette of pMV261. Prior to cloning into pMV261, it was necessary to clone the 5.0-kb segment into pUC18 to confirm the DNA sequences. Since we could not directly clone the 5.0-kb segment as one PCR-amplified fragment, three divided fragments were amplified from the genomic DNA of *M. avium* JATA51-01 by using following primers: GTFC-S and HA for the 2.0-kb PstI-HindIII fragment, HS and KA for the 1.0-kb HindIII-KpnI fragment, and KS and GTFD-A for the 2.0-kb KpnI-EcoRI fragment (Fig. 1A). These three fragments then were combined in pUC18 as a PstI-EcoRI fragment to give pUCgtfCD (Fig. 1A). A 5.0-kb PstI-EcoRI fragment was excised from pUCgtfCD and inserted into the PstI-EcoRI site of pMV261 to create pMVgtfCD, which expressed the above-described five genes (Fig. 1B).

Deletion of each gene from the *gtfC-gtfD* region was performed as follows. The expression vectors were constructed from pUCgtfCD by PCR using following primers: 18PST-U and MDHTA-S for the deletion of *gtfC*, MDHTA-U and MDHTA-D for the deletion of *mdhtA*, MERA-U and MERA-D for the deletion of *merA*, MTFF-U and MTFF-D for the deletion of *mtfF*, and MTFF-A and 18ECO-D for the deletion of *gtfD*. The PCR products were digested with each restriction enzyme and were ligated. The PstI-EcoRI fragment was excised from each resulting plasmid and was cloned into the same restriction sites of pMV261 to give pMVΔgtfC, pMVΔmdhtA, pMVΔmerA, pMVΔmtfF, and pMVΔgtfD (Fig. 1B).

The two *M. avium* genes *rtfA* and *gtfD* were amplified from genomic DNA of *M. avium* JATA51-01 by using the following primers: RTFA-S and RTFA-A for *rtfA* and GTFD-S and GTFD-PA for *gtfD*. The PCR products were digested with each restriction enzyme and were cloned into the corresponding site of pYM301 and pMV261 to give pYMrtfA-int and pMVgtfD, respectively.

To construct the vector for the simultaneous expression of *rtfA, mdhtA,* and *merA*, the HpaI site of pYMrtfA-int was replaced with an AflIII site by PCR using AFL-U and AFL-D to give pYMrtfA-int-Afl. The *mdhtA* and *merA* genes were amplified as one operon from genomic DNA of *M. avium* JATA51-01 by using the primers MDHTA-S2 and MERA-A. The PCR product was digested with

TABLE 2. Bacterial strains and vectors used in this study

Strain or vector	Characteristic(s)	Source or reference
Bacterial strains		
E. coli DH5α	Cloning host	
M. smegmatis mc²155	Expression host	25
M. avium JATA51-01 (ATCC 25291)	Source of the 5.0-kb region containing *gtfC, mdhtA, merA, mtfF,* and *gtfD*	
Vectors		
pUC18	*E. coli* cloning vector	
pBluescript II SK(+)	*E. coli* cloning vector	
pYM301	Site-specific integrating mycobacterial vector carrying the *hsp60* promoter cassette	This study
pYUB854	Source of pYM301	3
pMV306kan	Source of pYM301	24
pMV261	*E. coli-Mycobacterium* shuttle vector carrying the *hsp60* promoter cassette	27
pMVgtfCD	pMV261 with *gtfC, mdhtA, merA, mtfF,* and *gtfD*	This study
pMVΔgtfC	pMV261 with *mdhtA, merA, mtfF,* and *gtfD*	This study
pMVΔmdhtA	pMV261 with *gtfC, merA, mtfF,* and *gtfD*	This study
pMVΔmerA	pMV261 with *gtfC, mdhtA, mtfF,* and *gtfD*	This study
pMVΔmtfF	pMV261 with *gtfC, mdhtA, merA,* and *gtfD*	This study
pMVΔgtfD	pMV261 with *gtfC, mdhtA, merA,* and *mtfF*	This study
pMVgtfD	pMV261 with *gtfD*	This study
pYMrtfA-int	pYM301 with *rtfA*	This study
pYMrtfA-mdhtA-merA-int	pYM301 with *rtfA, mdhtA,* and *merA*	This study

A

GTFC-S   HA HS   KA   KS   GTFD-A

P   H   H   K   K   E

| 2.0-kb | | 1.0-kb | | 2.0-kb |

P   H   K   P K   E

| 3.0-kb | | 2.0-kb |

pBluescript II SK (+) with
Pst I-*Kpn* I fragment

pUC18 with
Kpn I-*EcoR* I fragment

P   H   K

| 3.0-kb |

P   H   K   E

| 5.0-kb |

gtfC   *mdhtA*   *merA*   *mtfF*   *gtfD*

pUCgtfCD

B

P   H   K   E

P_{hsp60} *gtfC*   *mdhtA*   *merA*   *mtfF*   *gtfD*   terminator

pMVgtfCD   P   ...   mdhtA   merA   mtfF   gtfD   T

pMVΔgtfC

pMVΔmdhtA
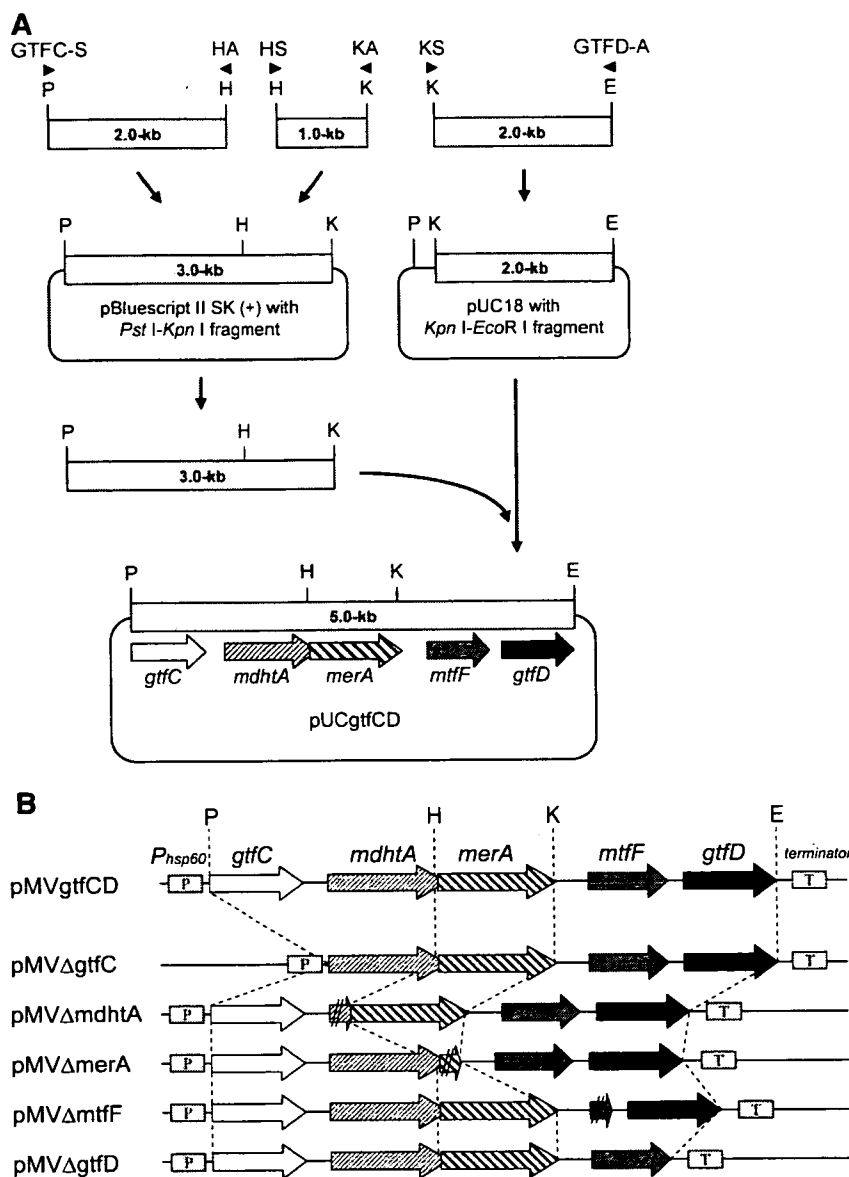
pMVΔmerA

pMVΔmtfF

pMVΔgtfD

FIG. 1. Schematic presentation of the cloning procedure for the 5.0-kb *gtfC-gtfD* region (A) and its gene-deleted constructs, which were inserted into an expression cassette made up of the *hsp60* promoter and the terminator of pMV261 (B). The primers used for PCR amplification of the three fragments are indicated by filled triangles. In pMVΔgtfC and pMVΔgtfD, the genes *gtfC* and *gtfD* were completely deleted from the *gtfC-gtfD* region of pMVgtfCD. In-frame deletions were designed for the construction of the expression cassettes of pMVΔmdhtA, pMVΔmerA, and pMVΔmtfF to prevent the polar effect on each downstream gene. P, PstI; H, HindIII; K, KpnI; E, EcoRI.

each restriction enzyme and cloned into the PstI-AflII site of pYMrtfA-int-Afl to give pYMrtfA-mdhtA-merA-int.

Isolation and purification of GPLs. Whole-lipid extracts were isolated from harvested bacterial cells that had been mixed with $CHCl_3$-CH_3OH (2:1, vol/vol) for several hours at room temperature. The extracts obtained from the organic phase were separated from the aqueous phase and evaporated to dryness. To remove the lipid components except for GPLs, the whole-lipid extracts were subjected to mild alkaline hydrolysis as previously described (20, 21). For analytical thin-layer chromatography (TLC), crude GPLs from equal amounts of harvested bacterial cells were spotted on silica gel 60 plates (Merck) using $CHCl_3$-CH_3OH (9:1, vol/vol) as the solvent and were visualized by spraying with 10% H_2SO_4 and then charring. Purified GPLs were prepared from crude GPLs by preparative TLC on the same plates and were extracted from the bands corresponding to each GPL. Perdeuteriomethylation for determination of the linkage position of sugar moieties was carried out as previously described (7, 10, 14).

GC-MS and MALDI-TOF analyses. For the monosaccharide analysis, crude GPLs from equal amounts of harvested cells were hydrolyzed in 2 M trifluoroacetic acid (2 h, 120°C), and the released sugars were reduced with sodium tetradeuterborate and then were acetylated with pyridine-acetic anhydride (1:1, vol/vol) at room temperature overnight. The resulting alditol acetates were separated and analyzed by gas chromatography-mass spectrometry (GC-MS) on a TRACE DSQ (Thermo Electron) equipped with an SP-2380 column (SUPELCO) using helium gas. The temperature program was from 52 to 172°C with 40°C/min increments and then from 172 to 250°C with 3°C/min increments. To determine the total mass of the purified GPLs, matrix-assisted laser desorption ionization-time of flight (MALDI-TOF) mass spectra (in the positive mode) were acquired on a QSTAR XL (Applied Biosystems) with a pulse laser emitting at 337 nm. Samples mixed with 2,5-dihydroxybenzoic acid as the matrix were analyzed in the reflectron mode with an accelerating voltage of 20 kV and operating in positive-ion mode.
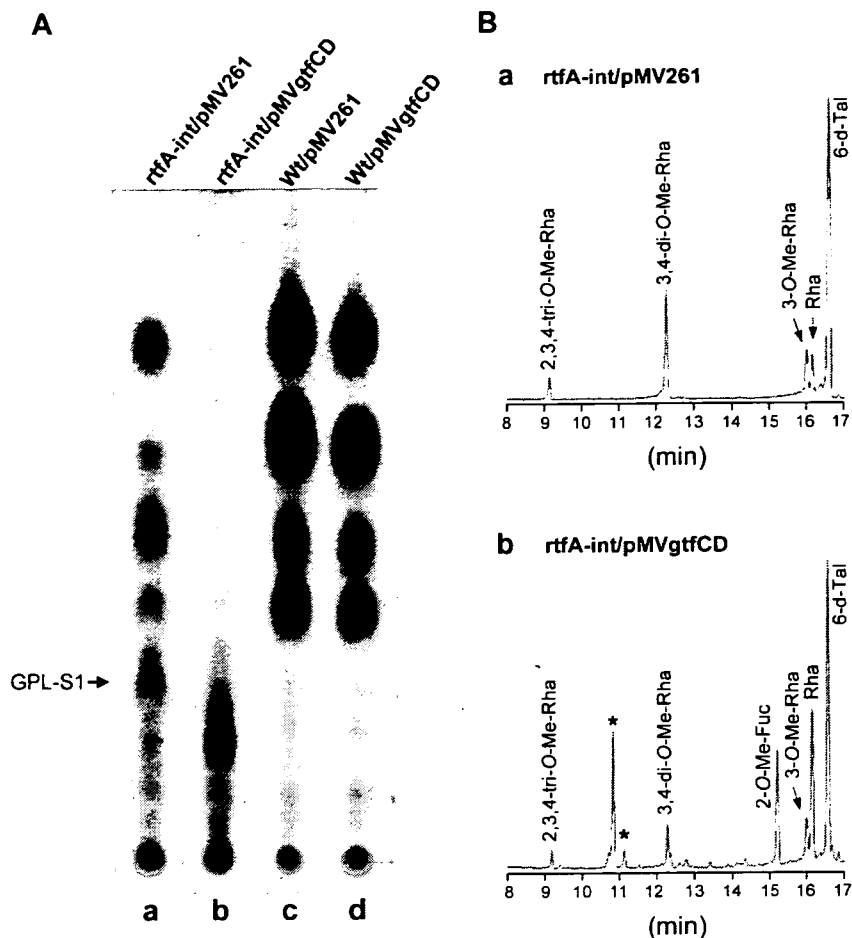
A

GPL-S1→

a b c d

B

a rtfA-int/pMV261

b rtfA-int/pMVgtfCD

FIG. 2. Functional analyses of the *gtfC-gtfD* region. (A) TLC analysis of crude GPL extracts from rtfA-int/pMV261 (lane a), rtfA-int/pMVgtfCD (lane b), Wt/pMV261 (lane c), and Wt/pMVgtfCD (lane d). The total lipid fraction after mild alkaline hydrolysis was spotted on plates and was developed in $CHCl_3$-CH_3OH (9:1 [vol/vol]). (B) GC-MS analyses of alditol acetates of sugars released from crude GPL extracts of rtfA-int/pMV261 (a) and rtfA-int/pMVgtfCD (b). Alditol acetate derivatives were prepared from the total lipid fraction after mild alkaline hydrolysis. Asterisks indicate noncarbohydrates.

RESULTS

Identification of the genes involved in the formation of the Fuc residue in serovar 2 GPL. To reveal the genes responsible for the fucosylation pathway that lead to the formation of serovar 2 GPL, we focused on the 5.0-kb segment designated the *gtfC-gtfD* region (GenBank accession no. AF125999.1). This region contains five genes: *mdhtA* and *merA*, whose deduced amino acid sequences show a high level of similarity to those of enzymes involved in Fuc synthesis; *mtfF*, previously identified as the fucosyl 2-*O*-methyltransferase gene; and *gtfC* and *gtfD*, putative glycosyltransferase genes whose functions remain unknown (13, 18). Since *M. smegmatis* only produces core GPLs, we introduced the chromosomal integrating vector pYMrtfA-int possessing the *M. avium* gene *rtfA*, whose gene product transfers the Rha residue to 6-d-Tal of core GPLs, and obtained the recombinant strain rtfA-int, which produces GPL with a terminal Rha residue (termed GPL-S1) that could be a substrate for the synthesis of serovar 2 GPL. The expression vector pMVgtfCD, harboring the *gtfC-gtfD* region (Fig. 1B), then was introduced into the GPL-S1-producing strain (rtfA-int) and wild-type mc²155, and GPL production was analyzed

by TLC (Fig. 2A). Although there were no differences between the TLC profiles of Wt/pMV261 and Wt/pMVgtfCD (Fig. 2A, lanes c and d), new spots appeared in rtfA-int/pMVgtfCD (Fig. 2A, lane b), indicating that the *gtfC-gtfD* region contains genes with the ability to convert GPL-S1 into structurally different compounds, but it can do so only in the presence of the *rtfA* gene. To confirm that the products formed in rtfA-int/pMVgtfCD contained Fuc, a characteristic of serovar 2 GPL, alkaline-stable extracts from rtfA-int/pMVgtfCD were hydrolyzed, and the released monosaccharides were analyzed by GC-MS (Fig. 2B). The results showed that 2-*O*-Me-Fuc, which is structurally related to serovar 2 GPL, was present together with Rha, 6-d-Tal, 3-*O*-Me-Rha, 3,4-di-*O*-Me-Rha, and 2,3,4-tri-*O*-Me-Rha in rtfA-int/pMVgtfCD (Fig. 2B, graph b). 2-*O*-Me-Fuc was not detected in strain rtfA-int/pMV261 (vector control) (Fig. 2B, graph a) or recombinant wild-type mc²155 (data not shown). These results indicated that the *gtfC-gtfD* region is responsible for the transfer of the Fuc residue to serovar 1 GPL. Additionally, for identification of the individual genes involved in this fucosylation, we constructed various plasmids that have one of the genes deleted from the *gtfC-gtfD* region, as shown in
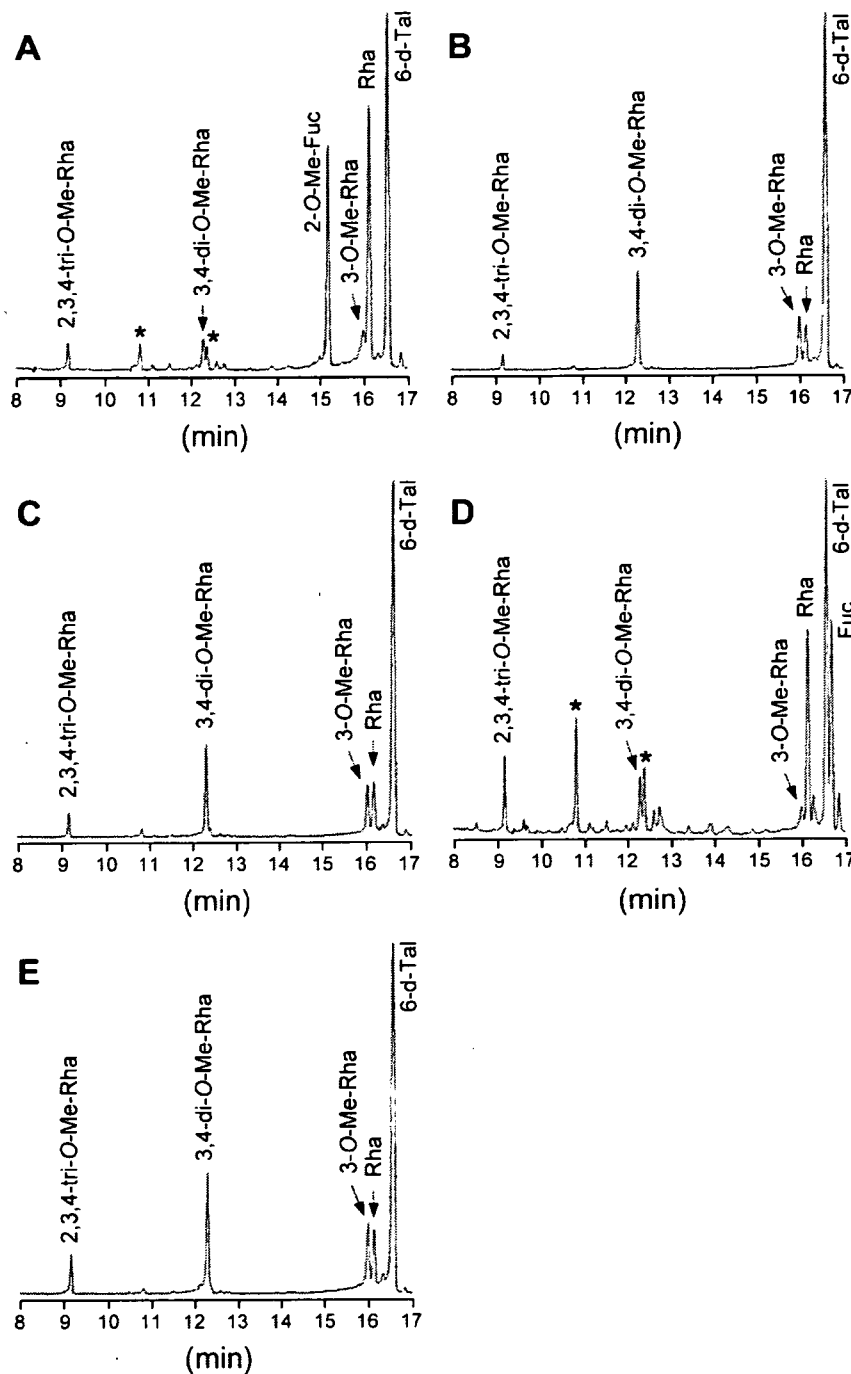
FIG. 3. GC-MS analyses of alditol acetates of sugars released from crude GPLs. GPLs were extracted from rtfA-int/pMVΔgtfC (A), rtfA-int/ pMVΔmdhtA (B), rtfA-int/pMVΔmerA (C), rtfA-int/pMVΔmtfF (D), and rtfA-int/pMVΔgtfD (E). Alditol acetate derivatives were prepared from the total lipid fraction after mild alkaline hydrolysis. Asterisks indicate noncarbohydrates.

Fig. 1B, and examined the sugar moieties of the alkaline-stable GPL extracts from each recombinant strain by GC-MS analysis (Fig. 3). The results show that the profile of rtfA-int/ pMVΔgtfC was the same as that of rtfA-int/pMVgtfCD, indicating that the *gtfC* gene does not participate in the formation of 2-O-Me-Fuc (Fig. 2B, graph b, and 3A). In rtfA-int/ pMVΔmtfF, Fuc was detected instead of 2-O-Me-Fuc, demonstrating that the *mtfF* gene encodes fucosyl 2-O-methyltrans-

ferase (Fig. 3D). On the other hand, no Fuc derivatives were detected in the recombinant strains rtfA-int/pMVΔmdhtA, rtfA-int/pMVΔmerA, and rtfA-int/pMVΔgtfD (Fig. 3B, C, and E). These results indicated that the three genes *mdhtA*, *merA*, and *gtfD* are all indispensable for the formation of the Fuc residue in serovar 2 GPL.

Functional analysis of the *gtfD* gene. Although the *gtfD* gene was predicted to encode a type of glycosyltransferase based on
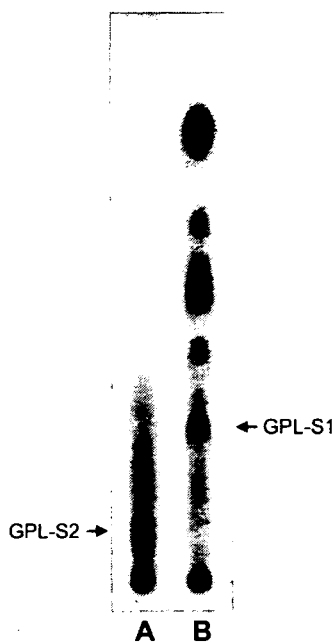
FIG. 4. TLC analyses of crude GPL extracts from rtfA-mdhtA-merA-int/pMVgtfD (lane A) and rtfA-mdhtA-merA-int/pMV261 (lane B). The total lipid fraction after mild alkaline hydrolysis was spotted onto plates and developed in CHCl₃-CH₃OH (9:1 [vol/vol]).

a homology search of its deduced amino acid sequences, it is not clear whether the product of *gtfD* functions as the glycosyltransferase that transfers the Fuc residue via 1→3 linkage to the Rha residue of serovar 1 GPL to form the oligosaccharide part of serovar 2 GPL. To elucidate the function of *gtfD*, we constructed a recombinant strain by introducing a chromosomal integrating vector expressing *rtfA*, *mdhtA*, and *merA* (pYMrtfA-mdhtA-merA-int). We then characterized the product formed when *gtfD* was expressed solely by the plasmid vector (pMVgtfD). TLC analysis of the recombinant strains showed that the *gtfD*-expressing strain (rtfA-mdhtA-merA-int/pMVgtfD) caused the appearance of a new spot, termed GPL-S2, in connection with the disappearance of GPL-S1 (Fig. 4, lane A), while the vector control (rtfA-mdhtA-merA-int/pMV261) did not produce GPL-S2 (Fig. 4, lane B). To determine the structure of sugar moieties of GPL-S2, perdeuteriomethylation was performed on purified GPL-S2, and derived alditol acetates were analyzed by GC-MS. The GC-MS profile yielded four peaks corresponding to 6-d-Tal, Rha, Fuc, and 2,3,4-tri-*O*-Me-Rha (data not shown). The characteristic spectra of Fuc, Rha, and 6-d-Tal are shown in Fig. 5. The spectrum of Fuc gave fragment ions at *m/z* of 121, 134, and 168, which represent the presence of deuteriomethyl groups at positions C-2, C-3, and C-4 (Fig. 5A). In contrast, the detection of fragment ions at *m/z* of 121, 134, 193, and 240 from Rha indicated that a deuteriomethyl group was introduced at positions C-2 and C-4 of Rha, whose C-3 position was acetylated (Fig. 5B). Additionally, positions C-3 and C-4 of 6-d-Tal were found to be deuteriomethylated, with the detection of fragment ions at *m/z* of 134, 181, and 193 (Fig. 5C). These observations demonstrated that position C-1 of Fuc is linked to position C-3 of Rha but not position C-2 of 6-d-Tal, because it

was previously determined that position C-1 of Rha is linked to position C-2 of 6-d-Tal in the oligosaccharide of serovar 1 GPL through the catalytic reaction of RtfA (14). Furthermore, we compared the molecular mass of GPL-S2 to that of GPL-S1 purified from the vector control strain by MALDI-TOF (mass spectrometry). The main pseudomolecular ion [M + Na]⁺ from both compounds revealed that the difference between GPL-S2 (*m/z*, 1,479.9) and GPL-S1 (*m/z*, 1,333.8) was 146 mass units, suggesting that a Fuc residue was further added to the GPL-S1 (data not shown). Accordingly, the structure of GPL-S2 was determined to have Fuc-(1→3)-Rha-(1→2)-6-d-Tal at D-*allo*-Thr and 2,3,4-tri-*O*-Me-Rha at D-alaninol (Fig. 6), demonstrating that *gtfD* encodes the glycosyltransferase that transfers a Fuc residue via 1→3 linkage to the Rha residue of serovar 1 GPL.

DISCUSSION

The gene cluster involved in synthesizing ssGPLs has been cloned from *M. avium* strains. In this cluster, the functions of several genes responsible for the biosynthesis of serovar 1 GPL, such as *rtfA*, *gtfA*, *gtfB*, *mtfB*, *mtfC*, and *mtfD*, have been elucidated (14, 16, 19). On the other hand, the genes associated with the conversion of serovar 1 GPL to other serotypes, including serovar 2 GPL, have not been identified. In this study, we focused on the five genes assumed to encode the enzymes associated with fucosylation in the biosynthesis of serovar 2 GPL and experimentally showed that GtfD is responsible for the transfer of the Fuc residue to the Rha residue of serovar 1 GPL (Fig. 6). Gene deletion experiments revealed that *mdhtA* and *merA* also contribute to the formation of the Fuc residue in serovar 2 GPL. The deduced amino acid sequences of *mdhtA* and *merA* showed high levels of similarity to GDP-D-mannose-4,6-dehydratase and GDP-6-deoxy-4-keto-D-mannose-3,5-epimerase-4-reductase, respectively. These are enzymes involved in the synthesis of L-Fuc from D-mannose and are highly conserved among other bacteria (1, 26). For mycobacteria, there are no homologues of *mdhtA* and *merA* in the genome databases for *M. bovis*, *M. leprae*, and *M. smegmatis*. However, for *M. tuberculosis*, the deduced amino acid sequences of Rv1511 and Rv1512 show 89 and 84% homology to those of *mdhtA* and *merA*, respectively. This observation is supported by the fact that several strains of *M. tuberculosis* produce the Fuc-containing phenolic glycolipid, whereas *M. bovis* and *M. leprae* lack the Fuc residue, and other carbohydrate components having the Fuc residue have not been reported from the above-mentioned three species. Thus, it is strongly suggested that *mdhtA* and *merA* encode synthetases involved in the conversion of D-mannose to L-Fuc that can be transferred by GtfD to form the Fuc residue of serovar 2 GPL (Fig. 6). Before performing the functional analyses of these genes, we speculated that the glycosyltransferase involved in the fucosylation was encoded by *gtfC*, but not *gtfD*, from the observations that *gtfC* includes a putative glycosyltransferase motif and its homologue in *M. tuberculosis*, Rv1514c, is adjacent to Rv1511 and Rv1512, which are predicted to be responsible for the Fuc synthesis, while a *gtfD* homologue, Rv2957, is located far from Rv1511, Rv1512, and Rv1514c. However, the deletion analysis demonstrated that *gtfC* does not contribute to the fucosylation of the GPLs. This result raises the possibility
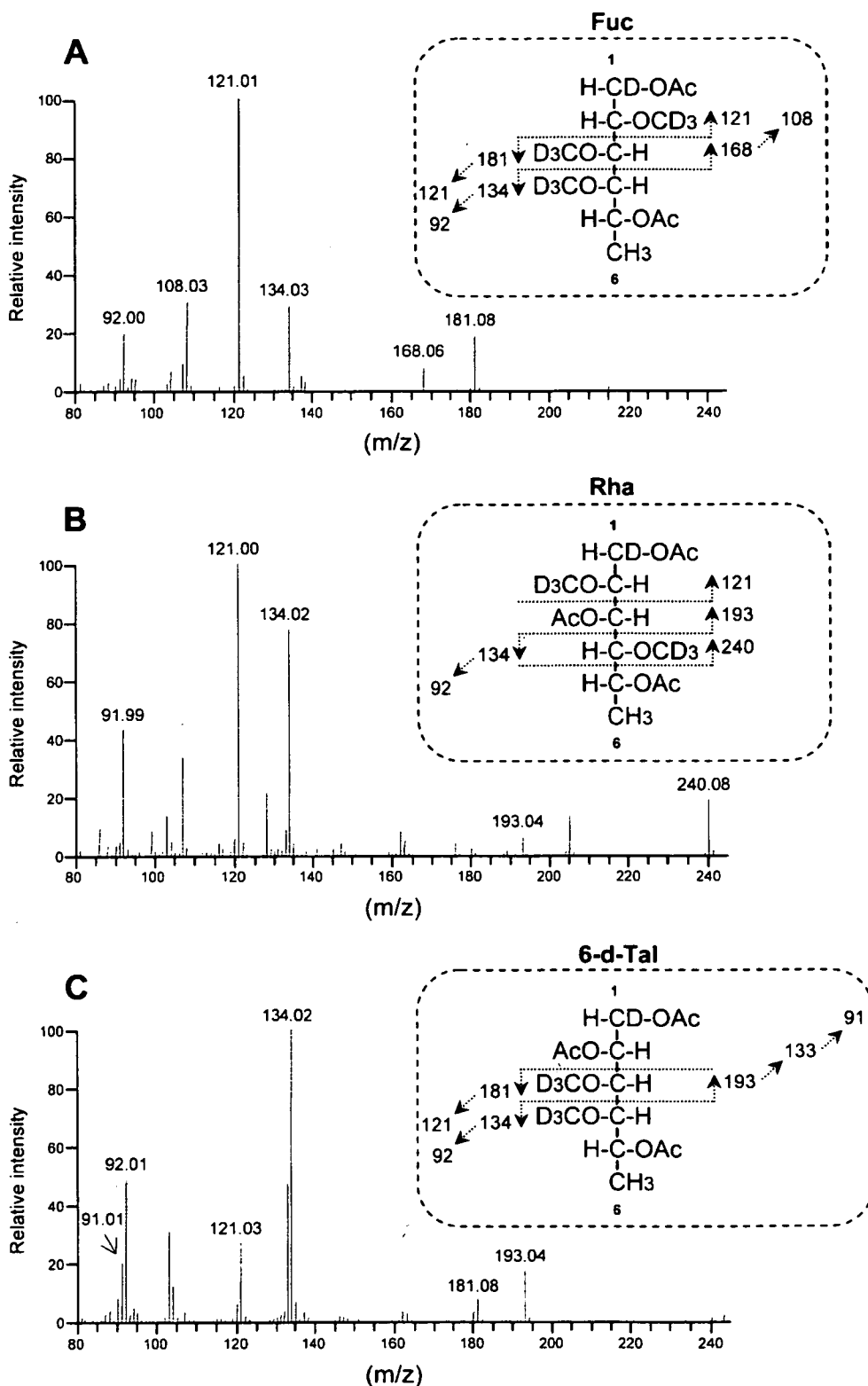
FIG. 5. GC mass spectra and fragment ion assignment of Fuc (A), Rha (B), and 6-d-Tal (C), which are derived from alditol acetates of sugars released from deuteriomethylated GPL-S2. Ac, acetate; D, deuterium.

that *gtfC* is involved in the transfer of another sugar moiety, such as glucuronic acid and Rha, followed by fucosylation, as observed for the serovar 3, 9, and 4 GPLs (9). As for *gtfD*, Rv2957 is reported to be one of the glycosyltransferase genes

involved in the biosynthesis of phenolic glycolipid in *M. tuberculosis*, but its catalytic functions, such as sugar substrate and glycosidic linkage, are not clear (22). Thus, our findings implied that Rv2957 is the fucosyltransferase gene responsible for
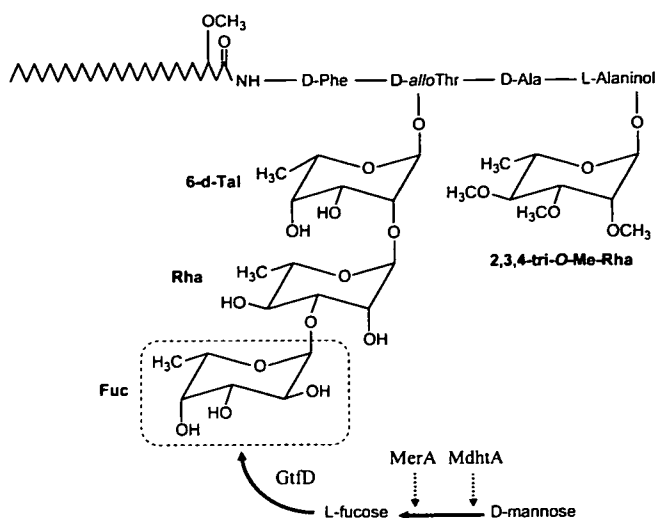
FIG. 6. Proposed structure and biosynthetic pathway of fucosylated GPL (GPL-S2).

the transfer of the Fuc residue in the phenolic glycolipid. Moreover, morphological observations showed that the surface of colony of the GPL-S2-producing strain was rougher than that of the vector control strain, suggesting that the presence of a Fuc residue in the GPL structure affected the cell surface properties (data not shown). Taking the results together, our study is the first report identifying the genes involved in the fucosylation pathway in mycobacteria and might provide a clue to understanding its role in the biosynthesis of glycolipids, including GPLs.

ACKNOWLEDGMENT

REFERENCES

1. Andrianopoulos, K., L. Wang, and P. R. Reeves. 1998. Identification of the fucose synthetase gene in the colanic acid gene cluster of Escherichia coli K-12. J. Bacteriol. 180:998–1001.
2. Aspinall, G. O., D. Chatterjee, and P. J. Brennan. 1995. The variable surface glycolipids of mycobacteria: structures, synthesis of epitopes, and biological properties. Adv. Carbohydr. Chem. Biochem. 51:169–242.
3. Bardarov, S., S. Bardarov, Jr., M. S. Pavelka, Jr., V. Sambandamurthy, M. Larsen, J. Tufariello, J. Chan, G. Hatfull, and W. R. Jacobs, Jr. 2002. Specialized transduction: an efficient method for generating marked and unmarked targeted gene disruptions in Mycobacterium tuberculosis, M. bovis BCG, and M. smegmatis. Microbiology 148:3007–3017.
4. Belisle, J. T., K. Klaczkiewicz, P. J. Brennan, W. R. Jacobs, Jr., and J. M. Inamine. 1993. Rough morphological variants of Mycobacterium avium. Characterization of genomic deletions resulting in the loss of glycopeptido-lipid expression. J. Biol. Chem. 268:10517–10523.
5. Belisle, J. T., L. Pascopella, J. M. Inamine, P. J. Brennan, and W. R. Jacobs, Jr. 1991. Isolation and expression of a gene cluster responsible for biosynthesis of the glycopeptidolipid antigens of Mycobacterium avium. J. Bacteriol. 173:6991–6997.
6. Billman-Jacobe, H., M. J. McConville, R. E. Haites, S. Kovacevic, and R. L. Coppel. 1999. Identification of a peptide synthetase involved in the biosynthesis of glycopeptidolipids of Mycobacterium smegmatis. Mol. Microbiol. 33:1244–1253.
7. Bjorndal, H., C. G. Hellerqvist, B. Lindberg, and S. Svensson. 1970. Gas-

8. Brennan, P. J., and H. Nikaido. 1995. The envelope of mycobacteria. Annu. Rev. Biochem. 64:29–63.
9. Chatterjee, D., and K. H. Khoo. 2001. The surface glycopeptidolipids of mycobacteria: structures and biological properties. Cell. Mol. Life Sci. 58:2018–2042.
10. Ciucanu, I., and F. Kerek. 1984. A simple and rapid method for the permethylation of carbohydrates. Carbohydr. Res. 131:209–217.
11. Daffe, M., and P. Draper. 1998. The envelope layers of mycobacteria with reference to their pathogenicity. Adv. Microb. Physiol. 39:131–203.
12. Daffe, M., M. A. Laneelle, and G. Puzo. 1983. Structural elucidation by field desorption and electron-impact mass spectrometry of the C-mycosides isolated from Mycobacterium smegmatis. Biochim. Biophys. Acta 751:439–443.
13. Eckstein, T. M., J. T. Belisle, and J. M. Inamine. 2003. Proposed pathway for the biosynthesis of serovar-specific glycopeptidolipids in Mycobacterium avium serovar 2. Microbiology 149:2797–2807.
14. Eckstein, T. M., F. S. Silbaq, D. Chatterjee, N. J. Kelly, P. J. Brennan, and J. T. Belisle. 1998. Identification and recombinant expression of a Mycobacterium avium rhamnosyltransferase gene (rtfA) involved in glycopeptidolipid biosynthesis. J. Bacteriol. 180:5567–5573.
15. Jeevarajah, D., J. H. Patterson, M. J. McConville, and H. Billman-Jacobe. 2002. Modification of glycopeptidolipids by an O-methyltransferase of Mycobacterium smegmatis. Microbiology 148:3079–3087.
16. Jeevarajah, D., J. H. Patterson, E. Taig, T. Sargeant, M. J. McConville, and H. Billman-Jacobe. 2004. Methylation of GPLs in Mycobacterium smegmatis and Mycobacterium avium. J. Bacteriol. 186:6792–6799.
17. Julander, I., S. Hoffner, B. Petrini, and L. Ostlund. 1996. Multiple serovars of Mycobacterium avium complex in patients with AIDS. APMIS 104:318–320.
18. Mills, J. A., M. R. McNeil, J. T. Belisle, W. R. Jacobs, Jr., and P. J. Brennan. 1994. Loci of Mycobacterium avium ser2 gene cluster and their functions. J. Bacteriol. 176:4803–4808.
19. Miyamoto, Y., T. Mukai, N. Nakata, Y. Maeda, M. Kai, T. Naka, I. Yano, and M. Makino. 2006. Identification and characterization of the genes involved in glycosylation pathways of mycobacterial glycopeptidolipid biosynthesis. J. Bacteriol. 188:86–95.
20. Miyamoto, Y., T. Mukai, F. Takeshita, N. Nakata, Y. Maeda, M. Kai, and M. Makino. 2004. Aggregation of mycobacteria caused by disruption of fibronectin-attachment protein-encoding gene. FEMS Microbiol. Lett. 236:227–234.
21. Patterson, J. H., M. J. McConville, R. E. Haites, R. L. Coppel, and H. Billman-Jacobe. 2000. Identification of a methyltransferase from Mycobacterium smegmatis involved in glycopeptidolipid synthesis. J. Biol. Chem. 275:24900–24906.
22. Perez, E., P. Constant, A. Lemassu, F. Laval, M. Daffe, and C. Guilhot. 2004. Characterization of three glycosyltransferases involved in the biosynthesis of the phenolic glycolipid antigens from the Mycobacterium tuberculosis complex. J. Biol. Chem. 279:42574–42583.
23. Recht, J., and R. Kolter. 2001. Glycopeptidolipid acetylation affects sliding motility and biofilm formation in Mycobacterium smegmatis. J. Bacteriol. 183:5718–5724.
24. Sambandamurthy, V. K., X. Wang, B. Chen, R. G. Russell, S. Derrick, F. M. Collins, S. L. Morris, and W. R. Jacobs, Jr. 2002. A pantothenate auxotroph of Mycobacterium tuberculosis is highly attenuated and protects mice against tuberculosis. Nat. Med. 8:1171–1174.
25. Snapper, S. B., R. E. Melton, S. Mustafa, T. Kieser, and W. R. Jacobs, Jr. 1990. Isolation and characterization of efficient plasmid transformation mutants of Mycobacterium smegmatis. Mol. Microbiol. 4:1911–1919.
26. Stevenson, G., K. Andrianopoulos, M. Hobbs, and P. R. Reeves. 1996. Organization of the Escherichia coli K-12 gene cluster responsible for production of the extracellular polysaccharide colanic acid. J. Bacteriol. 178:4885–4893.
27. Stover, C. K., V. F. de la Cruz, T. R. Fuerst, J. E. Burlein, L. A. Benson, L. T. Bennett, G. P. Bansal, J. F. Young, M. H. Lee, G. F. Hatfull, S. B. Snapper, R. G. Barletta, W. R. Jacobs, Jr., and B. R. Bloom. 1991. New use of BCG for recombinant vaccines. Nature 351:456–460.
28. Sweet, L., and J. S. Schorey. 2006. Glycopeptidolipids from Mycobacterium avium promote macrophage activation in a TLR2- and MyD88-dependent manner. J. Leukoc. Biol. 80:415–423.
29. Vergne, I., and M. Daffe. 1998. Interaction of mycobacterial glycolipids with host cells. Front. Biosci. 3:d865–876.
30. Yakrus, M. A., and R. C. Good. 1990. Geographic distribution, frequency, and specimen source of Mycobacterium avium complex serotypes isolated from patients with acquired immunodeficiency syndrome. J. Clin. Microbiol. 28:926–929.

Use of Protein Antigens for Early Serological Diagnosis of Leprosy[▽]

Malcolm S. Duthie,[1]* Wakako Goto,[1] Greg C. Ireton,[1] Stephen T. Reece,[1] Ludimila P. V. Cardoso,[2]
Celina M. T. Martelli,[2] Mariane M. A. Stefani,[2] Maria Nakatani,[3] Robson Crusue de Jesus,[3]
Eduardo M. Netto,[3] Ma V. F. Balagon,[4] Esterlina Tan,[4] Robert H. Gelber,[4]
Yumi Maeda,[5] Masahiko Makino,[5] Dan Hoft,[6] and Steven G. Reed[1]

*Infectious Disease Research Institute, 1124 Columbia St., Suite 400, Seattle, Washington 98104[1]; Tropical Pathology and
Public Health Institute, Federal University of Goiás, Goiânia, Brazil[2]; Federal University of Bahia, Salvador, Brazil[3];
Leonard Wood Memorial Center for Leprosy Research, Cebu City, Philippines[4]; Department of Microbiology,
Leprosy Research Center, National Institute of Infectious Diseases, Tokyo, Japan[5]; and Department of
Microbiology and Immunology, St. Louis University, St. Louis, Missouri 63110[6]*

Leprosy is a chronic and debilitating human disease caused by infection with the *Mycobacterium leprae*
bacillus. Despite the marked reduction in the number of registered worldwide leprosy cases as a result of the
widespread use of multidrug therapy, the number of new cases detected each year remains relatively stable.
This indicates that *M. leprae* is still being transmitted and that, without earlier diagnosis, *M. leprae* infection
will continue to pose a health problem. Current diagnostic techniques, based on the appearance of clinical
symptoms or of immunoglobulin M (IgM) antibodies that recognize the bacterial phenolic glycolipid I, are
unable to reliably identify early-stage leprosy. In this study we examine the ability of IgG within leprosy patient
sera to bind several *M. leprae* protein antigens. As expected, multibacillary leprosy patients provided stronger
responses than paucibacillary leprosy patients. We demonstrate that the geographic locations of the patients
can influence the antigens they recognize but that ML0405 and ML2331 are recognized by sera from diverse
regions (the Philippines, coastal and central Brazil, and Japan). A fusion construct of these two proteins
(designated leprosy IDRI diagnostic 1 [LID-1]) retained the diagnostic activity of the component antigens.
Upon testing against a panel of prospective sera from individuals who developed leprosy, we determined that
LID-1 was capable of diagnosing leprosy 6 to 8 months before the onset of clinical symptoms. A serological
diagnostic test capable of identifying and allowing treatment of early-stage leprosy could reduce transmission,
prevent functional disabilities and stigmatizing deformities, and facilitate leprosy eradication.

Cases in which *Mycobacterium leprae* infection manifests to
cause leprosy present as a bacteriologic, clinical, immunologic,
and pathological spectrum ranging from the extremes observed
in paucibacillary (PB) and multibacillary (MB) patients (21,
24). PB patients have one or a few skin lesions and a low or
absent bacterial index (BI; a measure of the number of acid-
fast bacilli in the dermis, expressed on a logarithmic scale) and
demonstrate specific cell-mediated immunity against *M. leprae*,
but they have low or absent titers of *M. leprae*-specific antibod-
ies and a granulomatous dermatopathology. In marked con-
trast, MB patients have multiple symmetric skin lesions and a
high BI and demonstrate high titers of anti-*M. leprae* antibod-
ies but an absence of specific cell-mediated immunity and a
dermatopathology largely devoid of functional lymphocytes
(21). Despite the implementation of a WHO-directed eradica-
tion program over the last 20 years, the worldwide annual rate
of new case detection for leprosy remains stable at approxi-
mately 300,000 (17, 18, 26, 27). Earlier and objective diagnosis
of leprosy could interrupt transmission and, in the long term,
help further reduce the number of new cases and facilitate
eradication.

There is no single diagnostic laboratory test for leprosy, and

diagnosis remains essentially clinical. Clinical diagnosis of lep-
rosy is dependent upon recognition of disease symptoms and is
therefore only possible once the disease has manifested. WHO
experts have listed diagnostic criteria as one or more of the
following: hypopigmented or reddish skin patches with definite
loss of sensation; thickened peripheral nerves; acid-fast bacilli
on skin smears/biopsy specimens (WHO Expert Committee on
Leprosy, 1998). Pure neuritic leprosy forms, however, present
with no skin lesion. Confounding WHO's implementation of a
global leprosy eradication strategy is that the number of
trained leprologists has diminished. This is inadvertently in-
creasing the likelihood that a clinical diagnosis is delayed or
even missed, especially in regions where leprosy has been con-
trolled (1, 13, 16, 25).

The presence of serum immunoglobulin M (IgM) antibody to
phenolic glycolipid I (PGL-I) correlates with BI in leprosy pa-
tients and has been used to support disease symptoms as a means
to categorize leprosy patients. Enzyme-linked immunosorbent as-
say (ELISA) and rapid lateral flow test formats have been devel-
oped for the detection of anti-PGL-I antibody (3, 4, 8, 19, 22, 23,
28). In one study, a lateral flow assay correctly diagnosed 97.4%
of MB patients, with a specificity of 86.2% (4). Patients toward
the PB end of the leprosy spectrum have low or no BI, however,
and the majority of these patients are not identified by PGL-I-
based tests (4, 7, 19). In addition, false-positive results in areas of
endemicity are relatively high (>10%) (4, 7, 19). Consequently,
none of these PGL-I-based tests has been widely implemented in

* Corresponding author. Mailing address: Infectious Disease Research
Institute, 1124 Columbia St., Suite 400, Seattle, WA 98104. Phone: (206)
330-2517. Fax: (206) 381-3678. E-mail: mduthie@idri.org.

field situations. In addition, many studies have demonstrated that MB patients have high titers of *M. leprae*-specific antibodies but PB patients have low or absent titers. For these reasons, the potential for serological diagnosis of low-BI patients, such as PB patients or MB patients who are developing disease, has not been thoroughly pursued.

In a recent small-scale study, we demonstrated that the ML0405 and ML2331 proteins were recognized by sera from MB leprosy patients presenting with high BI (20). In the current study we demonstrate that ML0405 and ML2331 are diagnostically relevant antigens by analyzing a large panel of MB leprosy patient sera from a variety of leprosy-affected regions (the Philippines, central and coastal Brazil, and Japan). We also examine the ability of *M. leprae* protein antigens to diagnose low-BI leprosy (PB patients and early MB patients) and show here the diagnostic potential of ML0405, ML2331, and a newly discovered *M. leprae* antigen, ML1556c. Based on the results, we construct and evaluate a fusion protein comprising ML0405 and ML2331 (designated leprosy IDRI diagnostic 1 [LID-1]) and demonstrate that this construct can be used to serologically diagnose leprosy patients among presymptomatic individuals, that is, before a clinical diagnosis is possible. Moreover, ML1556c may be a valuable adduct to LID-1 for the diagnosis of PB leprosy.

MATERIALS AND METHODS

Subjects and samples. Sera were obtained from patients with leprosy (MB and PB) or tuberculosis (TB), healthy household contacts of MB leprosy patients (HHC), and endemic and nonendemic controls (EC and NEC). MB and PB leprosy patient sera used in this study were derived from recently diagnosed, previously untreated individuals who did not have signs of reversal reactions. Leprosy was classified in each case by bacterial, histological, and clinical observations carried out by qualified personnel, with the BI recorded at the time of diagnosis. HHC were defined as adults living in the same house as an MB index case for at least 6 months. TB patients were included to evaluate potential antigen cross-reactivity with other mycobacterial infection. Sera from TB patients were obtained after drawing blood from *Mycobacterium tuberculosis* sputum-positive, human immunodeficiency virus-negative individuals with clinically confirmed pulmonary TB who were undergoing treatment. Normal sera (EC and NEC) were obtained after blood draws from volunteers with no history of leprosy or TB infection. In all cases, drawing of blood was carried out with informed consent (with local institutional review board approval or local ethics committee approval in Brazil, Japan, the Philippines, Seattle, and St. Louis). The composition of each study population is summarized in Table 1.

In Cebu City, leprosy and TB patients were recruited at the Cebu skin clinic and Leonard Wood Memorial Research Center in Cebu City, Cebu (Philippines) from 2003 to 2006. Between 1985 and 1991, sera were collected prospectively from individuals who resided with MB patients (BI > 2) for at least 2 years and were free of leprosy as determined by clinical dermato-neurological examination at the inclusion point of the study. Some of these individuals developed MB leprosy as the study progressed, and these sera have previously been described (11).

In Goiânia, the state capital of Goiás State (western central Brazil), leprosy and TB patients were recruited at the main outpatient clinics of Centro de Referência em Diagnóstico e Terapêutica and Hospital Anuar Auad in 2006. PB leprosy patients were selected from a cohort of leprosy patients with a single skin lesion recruited at Brazilian sites of endemicity from 1999 to 2001, as previously described (9).

In Salvador, the state capital of Bahia State (northeast coastal Brazil), leprosy patients were recruited at Hospital Dom Rodrigo de Menezes in 2006.

In Japan, leprosy patients were recruited at the National Sanatorium Oshimaseishoen, Kagawa.

In St. Louis, sera were collected from U.S.-based individuals at a variety of times following *Mycobacterium bovis* BCG immunization.

All serum specimens were aliquoted and stored at −20°C or −80°C prior to assay.

TABLE 1. Study populations

Site	Sample categorization (total no.)	BI (mean)	Sex ratio[a]	Mean age (yr) (range)
Cebu City, Philippines	MB (17)	2.8	2.4	30 (18–55)
	PB (54)	0.5	0.4	31 (15–45)
	TB (6)		5	45 (35–53)
	EC (8)		1	26 (19–38)
	HHC (10)		0.4	38 (18–60)
Goiânia, Brazil	MB (28)	2.4	1.5	44 (19–81)
	PB (83)	0	0.4	33 (7–76)
	TB (26)		2.7	39 (17–66)
	EC (30)		0.1	20 (19–26)
	HHC (11)		0.5	28 (18–51)
Salvador, Brazil	MB (10)	NA[b]	3.5	35.1 (20–70)
	PB (6)	0	5	31.6 (12–42)
	HHC (11)		0.1	48.5 (25–57)
Kagawa, Japan	MB (30)	NA	NA	60 (48–79)
	PB (30)	0	NA	70 (55–90)
	EC (26)		NA	54 (48–62)

[a] Male/female ratio.
[b] NA, not available.

Cloning and purification of target antigens. DNA encoding selected *M. leprae* proteins was PCR amplified from *M. leprae* Thai-53 genomic DNA using *Pfx* DNA polymerase (Invitrogen, Carlsbad, CA). PCR primers were designed to incorporate specific restriction enzyme sites 5′ and 3′ of the gene of interest and excluded in the target gene for directional cloning into the expression vector pET28a (Novagen, Madison, WI). After PCR amplification, purified PCR products were digested, ligated with vector DNA, and used to transform *Escherichia coli*, and individual clones were induced to produce recombinant proteins, as previously described (20). Recombinant proteins were quantified using the bicinchoninic acid protein assay (Pierce, Rockford, IL), and quality was assessed by sodium dodecyl sulfate-polyacrylamide gel electrophoresis. The characteristics of each *M. leprae* protein evaluated are summarized in Table 2. The ML1556c protein was included because portions of the ML1556 protein were identified in four separate clones during serological expression screening with sera from PB leprosy patients (data not shown) (20). Recognition of the clones was derived from amino acids 58 to 256 of ML1556, which are only 47% identical to the *M. tuberculosis* protein Rv2839 (compared to 82% identity across the entire amino acid sequences of ML1556 and Rv2839).

Determining patient reactivity by ELISA. ELISAs were conducted independently at IDRI, Seattle, WA (Cebu and St. Louis sera); UFG, Goiânia, and UFB, Salvador, Brazil; and NIID, Tokyo, Japan. Polysorp 96-well plates (Nunc, Rochester, NY) were coated with 1 μg/ml recombinant protein or 200 ng/ml of natural disaccharide with octyl linkage (NDO), the synthetically derived B-cell epitope of PGL-I, conjugated to bovine serum albumin (NDO-BSA; kindly supplied by John Spencer, Colorado State University, under NIH contract N01 AI-25469), in bicarbonate buffer overnight at 4°C and blocked for 1 h at room temperature with phosphate-buffered saline–Tween with 1% BSA on a plate shaker. Serum diluted appropriately in 0.1% BSA was added to each well, and plates were incubated at room temperature for 2 h with shaking. Plates were washed with buffer only, and horseradish peroxidase-conjugated IgG or IgM (Rockland Immunochemicals, Gilbertsville, PA), diluted in 0.1% BSA, was added to each well and incubated at room temperature for 1 h with shaking. After washing, plates were developed with peroxidase color substrate (Kirkegaard & Perry Laboratories, Gaithersburg, MD), and the reaction was quenched by the addition of 1 N H₂SO₄. The optical density (OD) of each well was read at 450 nm. Positive responses were defined as an OD of >2× the mean OD of endemic control sera or an OD of >0.1, whichever was higher.

Statistics. P values were determined using Student's t test.

RESULTS

Recognition of *M. leprae* proteins by Filipino leprosy patient sera. The majority of MB leprosy patients are readily identified

TABLE 2. Main characteristics of *M. leprae* antigens tested[a]

Gene accession no.	Functional classification[b]	Protein type	Length (bp)	Product size (kDa)	% Identity[c] with:				
					M. tuberculosis H37Rv[e]	*M. bovis* AF2122/97[e]	*M. avium* 104[d]	*M. marinum* ATCC BAA-535[e]	*M. smegmatis* MC2 155[d]
ML0091	II.C.2	28-kDa antigen precursor	711	23.7	53	53	54	54	48
ML0405	V	Conserved hypothetical	765	25.3	62	62	None	NA	None
ML1633	II.C.2	Possible secreted hydrolase	1,608	57.0	25	25	35	81	62
ML2055	IV.A	Probable cell surface protein	864	29.5	72	72	69	73	54
ML2331	II.C.2	Possible secreted protein	771	26.5	80	80	77	80	67
ML2346	VI	Hypothetical	906	33.9	None	None	None	None	None
ML1556	II.A.6	Translation initiation factor	2,775	96.6	84	82		90	

[a] Annotations for gene accession number, functional classification, and protein type are according to the Sanger database.

[b] Functional classifications: II.C.2, surface polysaccharides, lipopolysaccharides, proteins, and antigens; V, conserved hypotheticals; IV.A, virulence; VI, unknowns; II.A.6, protein translation and modification.

[c] BLAST reports were performed in September 2006; tBLASTn was used for comparisons of proteins versus translated DNA. NA, not applicable.

[d] From http://www.tigr.org.

[e] From http://www.sanger.ac.uk/Projects.

by ELISA and lateral flow tests, which assess the capacity of patient IgM to bind *M. leprae* PGL-I or its synthetic analogue (NDO) conjugated to a carrier protein (BSA). In comparison with MB leprosy patients, PB leprosy patients have low or no anti-PGL-I responses and are more difficult to diagnose serologically. We therefore sought to determine whether PB sera recognized protein antigens, expanding our previous analyses and comparing the potential of NDO-BSA, ML0405, and ML2331 to diagnose leprosy, and found that the protein antigens have a similar profile for leprosy diagnosis as that for NDO-BSA; all three test antigens were readily detected by MB patient sera, by some PB patient sera, and by few, if any, EC, HHC, or TB sera (Fig. 1). Thus, similar to NDO-BSA, ML0405 and ML2331 demonstrate good potentials for the diagnosis of leprosy.

Recognition of MB leprosy patient sera with refined ML0405 antigen constructs. To learn more regarding the se-

roreactivity of ML0405 and enhance recombinant ML0405 expression for purification, we expressed a variety of ML0405 polypeptide fragments and determined whether Filipino MB leprosy patient sera had similar binding capacities to these fragments and to full-length (ML0405FL) protein. All constructs were able to bind MB patient sera (Fig. 2) ($P < 0.01$ for MB versus EC). The reactivity of a truncated form (ML0405Tr) of the protein was equivalent to the reactivity of ML0405FL ($P = 0.885$ for MB patient sera), whereas the reactivity of the protein construct lacking the predicted membrane-spanning region (ML0405Tm) declined slightly (Fig. 2) ($P = 0.047$ and 0.060 for Tm versus FL and Tr forms, respectively, for MB). These data indicate that the majority, if not all, of the B-cell epitopes recognized by antibodies in patient sera are retained and accessible in the truncated form of the protein. Further testing was conducted using either ML0405FL or ML0405Tr.
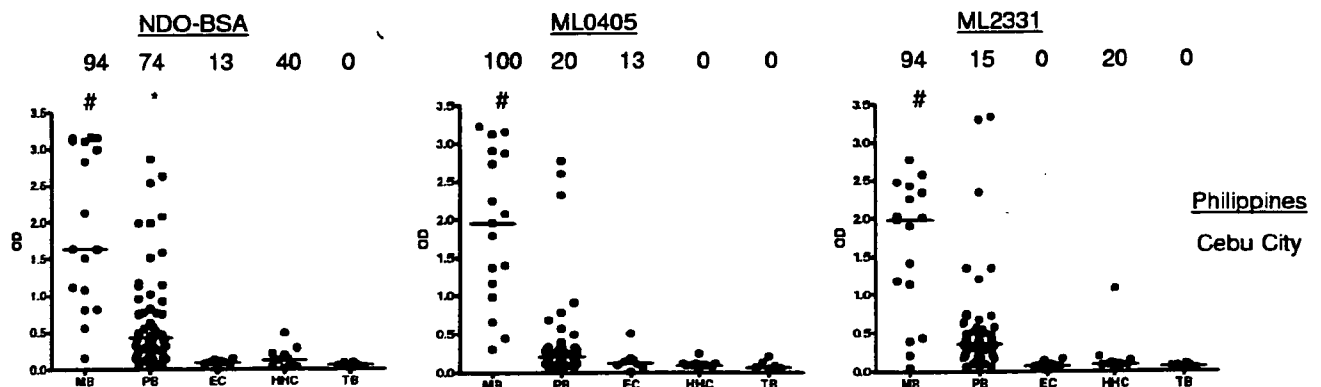

FIG. 1. Sera from Filipino leprosy patients react with recombinant *M. leprae* antigens. Sera from clinically diagnosed MB and PB leprosy patients, EC individuals, and HHC of MB leprosy patients were assessed against NDO-BSA, ML0405, and ML2331. NDO-BSA reactivity was assessed by IgM binding, and protein reactivity was assessed by IgG binding. Sera were from Cebu City, Philippines. Each point represents an individual serum sample, and the median is represented by the line. The number above each data set is the percent positive responses. *, $P < 0.05$; #, $P < 0.001$ versus EC.

ML0405FL 394aa

ML0405Tm 294aa (Δ 100-200)
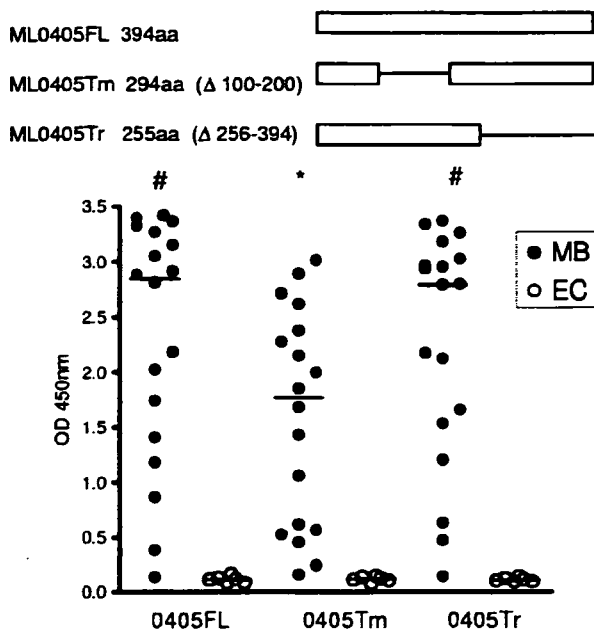
ML0405Tr 255aa (Δ 256-394)

FIG. 2. ML0405 constructs react with MB leprosy patient sera. Different ML0405 constructs were created and expressed as recombinant proteins. The schematic diagram shows the sequence alignment of each of these constructs, with the deleted regions indicated by the line. Each construct was tested for IgG reactivity by ELISA with individual Filipino MB leprosy patient sera ($n = 18$) or EC sera ($n = 6$). *, $P < 0.05$; #, $P < 0.001$ versus EC.

Diagnosis of Filipino PB leprosy patients with *M. leprae* proteins. We then went on to more closely investigate the potential of *M. leprae* antigens for diagnosing PB leprosy. Sera from Filipino patients clinically diagnosed with PB leprosy and with a low BI were tested for reactivity with potential diagnostic *M. leprae* antigens (ML0405Tr, ML2331, ML1556c, and NDO-BSA). NDO-BSA was capable of identifying 57% (26 of 46) of these Filipino PB leprosy patients, but a substantial number of samples provided weak positive responses (Fig. 3). ML0405 and ML2331 also reacted with sera from some PB patients (Fig. 3A and B). Most of these Filipino sera that reacted with these proteins also demonstrated strong NDO-BSA responses, however, and so the added benefit of using these antigens for leprosy diagnosis within the Filipino population appeared minimal. In contrast, 4 of 20 sera that were weak positive/negative by NDO-BSA ELISA testing demonstrated strong reactivity to ML1556c (Fig. 3C). This result suggests that ML1556c may be useful as an adjunct to PGL-I testing, or other tests, to improve the sensitivity and clarity of leprosy diagnosis.

To test the specificity of ML1556c as a leprosy diagnostic reagent, we directly compared the reactivities of ML1556c with sera from PB leprosy patients, MB leprosy patients, TB patients, EC, and HHC of MB leprosy patients located in Cebu City, Philippines (Fig. 3D). Positive responses were observed in five of eight additional PB leprosy sera tested, with three of the sera yielding strong responses that could provide a clear diagnosis. Positive responses to ML1556c were also observed in two of seven MB leprosy sera tested in this experiment.
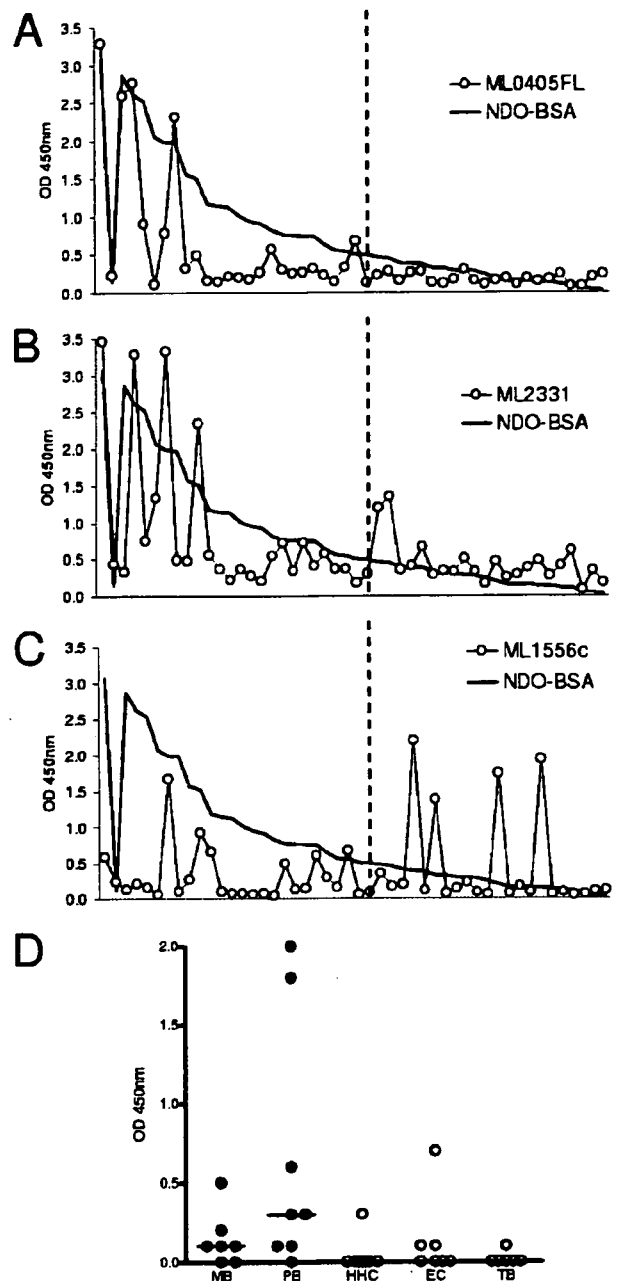

FIG. 3. *M. leprae* proteins react with PB leprosy patient sera. (A to C) Antibody reactivities of sera from a pool of clinically diagnosed MB leprosy patients, from a pool of negative control individuals, and from 46 clinically diagnosed PB leprosy patients were assessed against NDO-BSA and ML0405 (A), ML2331 (B), and ML1556c (C). NDO-BSA reactivity was assessed by IgM binding and, for reference, is shown in each plot. Recombinant protein reactivity was assessed by IgG binding. The first open circle represents the value obtained for pooled MB sera, while the next open circle represents the reactivity of pooled EC sera; individual PB sera are then arranged along the x axis according to their responsiveness versus NDO-BSA. The dashed line indicates the point at which diagnosis by NDO-BSA reactivity becomes unclear. ML1556c reacts with PB leprosy patient sera. (D) IgG reactivities of ML1556c with a small panel of individual sera from EC, leprosy patients (MB and PB), and TB patients were determined by ELISA using samples from Cebu City, Philippines. Each point represents an individual serum sample, and the median is represented by the line.
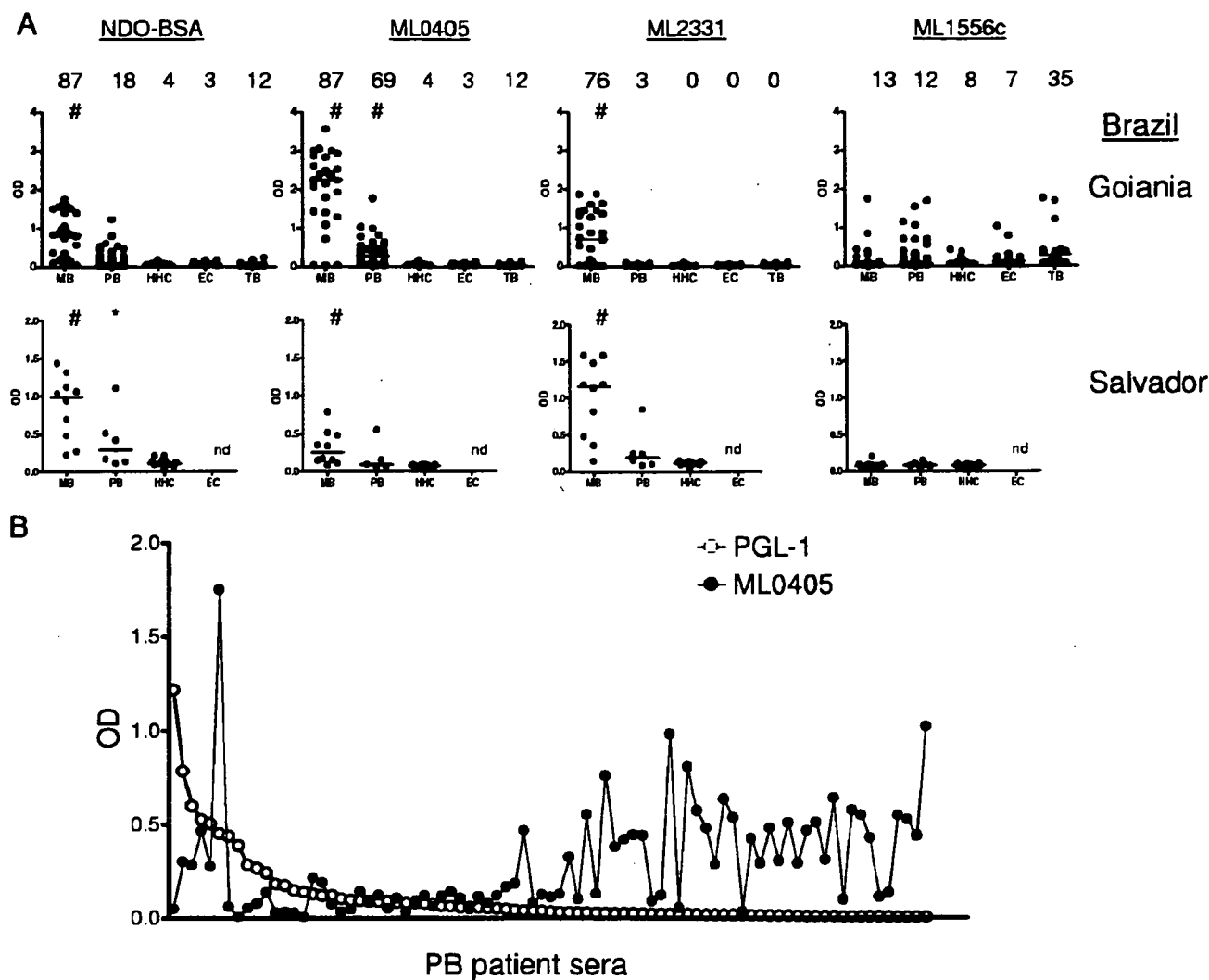
FIG. 4. Sera from Brazilian leprosy patients react with recombinant *M. leprae* antigens. Sera from clinically diagnosed MB and PB leprosy patients, EC individuals, and HHC of MB leprosy patients were assessed against NDO-BSA, ML0405, ML2331, and ML1556c. NDO-BSA reactivity was assessed by IgM binding, and protein reactivity was assessed by IgG binding. Sera were from Goiânia and Salvador (see Table 1). (A) Each point represents an individual serum sample, and the median is represented by the line. The number above each data set is the percent positive responses. *, $P < 0.05$; #, $P < 0.001$ versus EC. (B) To demonstrate complementarity, the individual PB sera from Goiânia are arranged along the x axis according to their responsiveness versus NDO-BSA and overlaid with the response of each serum to ML0405.

ML1556c did not react with any of the Filipino TB patient sera tested, was recognized by only one of eight HHC sera, and reacted with only one of six EC sera. Negative results were obtained upon further testing involving another 45 TB sera and 23 NEC sera (data not shown). Taken together, these results generated from sera from the Philippines suggested the utility of ML1556c to improve the diagnosis of PB leprosy.

Identification of leprosy patients in Brazil. We also examined the ability of recombinant *M. leprae* antigens to identify leprosy patients located around Goiânia, Brazil, and Salvador, Brazil. Within the clinically diagnosed leprosy population, PGL-I/NDO-BSA was capable of identifying 87% (33 of 38) of the MB patients (Fig. 4). In agreement with the results obtained by analysis of Filipino leprosy patient sera, ML0405 and ML2331 reacted with large proportions of Brazilian MB pa-

tient sera (87% [33 of 38] and 76% [29 of 38], respectively), and ML1556c reacted with only some MB patient sera (13%, 5 of 38) (Fig. 4). In Goiânia, positive responses were also observed against antigens ML0091 (71%, 20 of 28), ML1633 (32%, 9 of 28), ML2055 (75%, 21 of 28), and ML2346 (29%, 8 of 28) (data not shown). The clarity of MB leprosy diagnosis (strength of signal in positive samples versus negative samples) in Goiânia was greater when using ML0405 rather than NDO-BSA, but in Salvador it was greater when using ML2331 rather than NDO-BSA.

We also determined if these antigens were recognized by Brazilian PB patient sera. PGL-I/NDO-BSA was capable of identifying only 20% (18 of 89) of the PB patients, a level not appreciably higher than the proportion of positive responses observed with TB patients (12%, 3 of 26) (Fig. 4A). An IgG
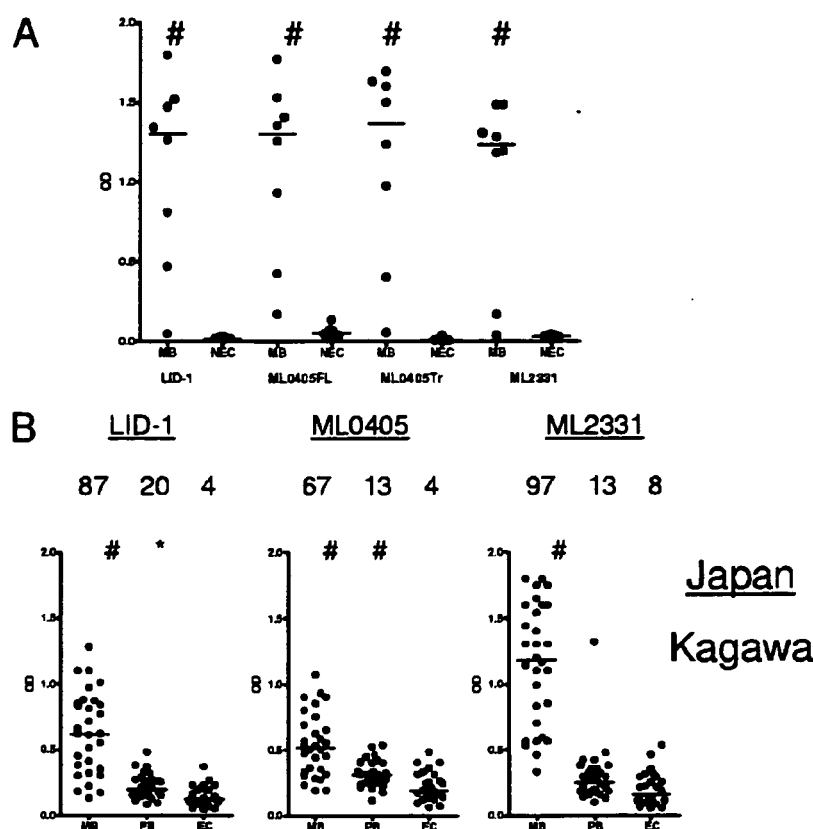
FIG. 5. LID-1 retains reactivity with leprosy patient sera. (A) LID-1 (a fusion construct of ML0405 and ML2331), ML0405FL, ML0405Tr, and ML2331 reactivities were assessed by IgG binding in an ELISA with eight MB leprosy patient serum samples from Salvador and eight NEC serum samples. (B) Sera from clinically diagnosed Japanese MB and PB leprosy patients, and Japanese EC individuals, were assessed for IgG reactivities with LID-1, ML0405, and ML2331. Each point represents an individual serum sample, and the median is represented by the line. The number above each data set is the percent positive responses. *, $P < 0.05$; #, $P < 0.001$ versus EC.

reactivity that permitted serologic diagnosis of an increased number of PB leprosy patients was observed for ML0405 (69%, 61 of 89), but responses to ML2331 were very weak, with very few positives (3%, 3 of 89) (Fig. 4A). The antigens ML0091 (6%, 5 of 83), ML1633 (17%, 14 of 83), ML2055 (13%, 11 of 83), and ML2346 (27%, 22 of 83) were recognized by some PB patient sera, but responses were generally weak (data not shown). Many of the PB patient sera that did not react with PGL-1 had a strong reactivity with ML0405 (Fig. 4B). ML1556c was recognized by only a minor subset of PB leprosy patient sera (12%, 11 of 89) and Brazilian EC individuals (6.7%, 2 of 30), but ML1556c reactivity was detected in a substantial number of Brazilian TB patients (35%, 9 of 26). These data indicate only a minor number of positive results in the Brazilian population if ML1556c is used for leprosy diagnosis, with a further complication of false-positive diagnosis in TB patients. Antigen ML0405, however, did not react with significant numbers of EC sera (3.3%, 1 of 30) or TB sera (12%, 3 of 26) (Fig. 4A). These results indicate that ML0405 can recognize some PB leprosy patients in the Brazilian population and could be used to augment leprosy diagnosis with PGL-1.

Construction of a fusion construct of ML0405-ML2331 (LID-1). Having extended our earlier observation that the sin-

gle antigens ML0405 and ML2331 have the potential to diagnose leprosy (20), and given the observations that ML0405 appeared better for diagnosis in Goiânia and Cebu City but ML2331 appeared better for diagnosis in Salvador, we constructed a single fusion molecule incorporating both proteins. ML0405Tr was expressed at the C terminus of the molecule and ML2331 in the N terminus. Following recombinant expression, we validated the reactivity of the construct by assaying LID-1 versus a small panel of sera from Salvador that had bound each single component. These sera readily detected LID-1, ML0405FL, ML0405Tr, and ML2331 (Fig. 5A). Importantly, construction of the fusion protein did not introduce false-positive results with NEC sera (Fig. 5A).

We further extended our examination of sera from different geographic locations by assessing sera from Japanese leprosy patients for reactivity with ML0405, ML2331, and LID-1. Positive response were observed with MB patient sera (67% [20 of 30] for ML0405, 97% [29 of 30] for ML2331, and 87% [26 of 30] for LID-1) and PB patient sera (13% [4 of 30] for ML0405, 13% [4 of 30] for ML2331, and 20% [6 of 30] for LID-1), with few responses in EC sera (4% [1 of 26] for ML0405, 8% [2 of 26] for ML2331, and 4% [1 of 26] for LID-1) (Fig. 5B). Taken together, these data indicate that LID-1 is useful as a diagnostic antigen for leprosy.
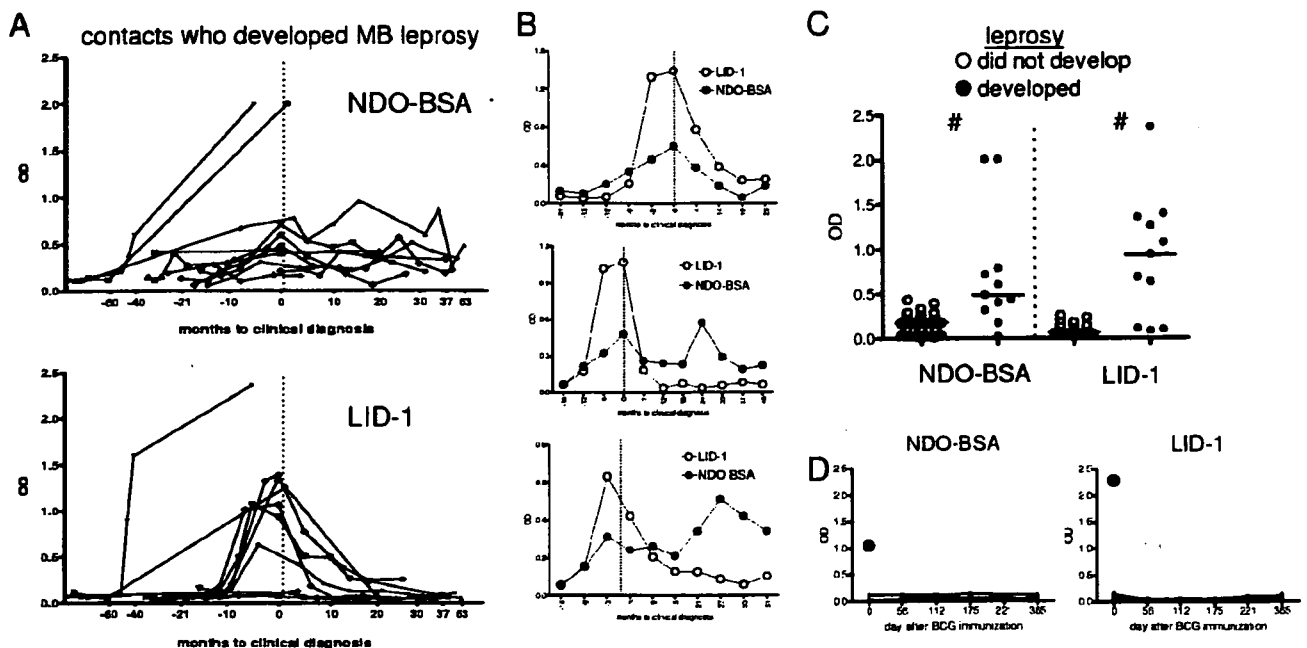
FIG. 6. LID-1 reactivity can diagnose leprosy before clinical symptoms. (A) LID-1 and NDO-BSA reactivities within sera from a prospective study conducted in Cebu City, Philippines, were assessed by either IgG or IgM binding in an ELISA. Sera were collected at a variety of times prior to the clinical diagnosis of MB leprosy in 11 patients and at a variety of times after the commencement of treatment. (B) Representative plots for individual patients are shown. (C) Sera were collected from 57 household contacts that did not develop clinical leprosy and were compared with single serum samples from each individual contact that developed leprosy (serum samples were collected within 3 months of clinical diagnosis). #, $P < 0.001$. (D) LID-1 and NDO-BSA reactivities within sera from a prospective study using 10 U.S.-based individuals who were immunized with BCG were assessed. Sera were collected at regular intervals following BCG immunization. The solid circle at day zero designates the reactivity of a leprosy patient serum sample that was included as a positive control.

LID-1 reactivity can diagnose leprosy before clinical symptoms. Having demonstrated that the LID-1 fusion molecule retained the ability to diagnose leprosy patients but lacked responses to EC sera, we obtained sera from a prospective study conducted in Cebu City, Philippines, between 1985 and 1991 (11). In that study, household contacts of leprosy patients were monitored over a prolonged period of time, and some developed clinical MB leprosy. In sera from the individuals who developed MB leprosy, as previously reported, anti-PGL-I levels increased before leprosy was diagnosed by clinical exam (Fig. 6A). Our data also indicate that anti-LID-1 antibody levels began to increase markedly as soon as 1 year prior to clinical diagnosis (Fig. 6A). For many of the patients (7 of 11, 64%) the increase in the anti-LID-1 IgG response was strikingly more obvious than the increase in the anti-PGL-I IgM response (Fig. 6B). Those patients that developed clinical leprosy had anti-PGL-1 antibody levels not dissimilar to many individuals who did not develop leprosy (Fig. 6C). The difference in anti-LID-1 antibody levels was much clearer, with a much larger differentiation between the positive responses of patients who developed leprosy compared with the extremely low levels of anti-LID-1 antibody in individuals who did not develop leprosy (Fig. 6C). Taken together, these data indicate that LID-1 is capable of providing an early serological diagnosis of leprosy.

LID-1 does not react with sera from individuals recently exposed to BCG. To examine in detail if leprosy diagnosis could be complicated by exposure to or infection with other mycobacteria, we also examined sera collected longitudinally from 10 U.S.-based individuals who were immunized with BCG. None of these BCG-immunized individuals developed positive serological responses against LID-1 or NDO-BSA (Fig. 6D). These data indicate that LID-1 can provide a clear diagnosis of *M. leprae* infection prior to the onset of signs that permit clinical leprosy diagnosis and that LID-1-based diagnostic tests could be used to expedite leprosy treatment.

DISCUSSION

Current diagnosis of leprosy is based on the appearance of clinical signs, and it is well established that the earlier a patient is identified the better their response to treatment. In addition, MB leprosy patient household contacts have a higher risk of developing clinical leprosy than contacts of PB leprosy patients (10, 12). This has been attributed to increased shedding and spreading of viable bacteria by MB leprosy patients (2). Accurate and early detection of *M. leprae*-infected individuals will open the possibility of earlier treatment that could both prevent disability and significantly reduce leprosy transmission.

We have evaluated the serological responses to a variety of *M. leprae* protein antigens in an attempt to discover antigens that can improve diagnosis of leprosy by detecting patients with a low BI (PB leprosy patients or early MB leprosy patients). We demonstrated that (i) ML0405 and ML2331 can be used to diagnose MB leprosy patients independently of geographic location; (ii) ML1556c can recognize some PB patients (al-

though it is recognized by some TB sera as well); (iii) ML0405 and ML2331 can be used for diagnosis of some PB patients; (iv) a fusion construct of ML0405 and ML2331 (LID-1) retains diagnostic capability; and (v) LID-1 can provide a clear leprosy diagnosis before the onset of clinical symptoms. These findings will improve both leprosy diagnosis and patient care.

One approach for the early detection of *M. leprae* infection is through serological diagnosis. We have conducted screening to identify *M. leprae* antigens that have not previously been described, and we then evaluated the diagnostic potential of these antigens with leprosy patient sera. In this study, the diagnostic potential of select antigens was assessed in clinically disparate leprosy patient groups, ranging from MB patients who presented with large bacterial burdens and large skin lesions to PB patients who presented with low or absent bacterial burdens and a few, small skin lesions. As expected, MB leprosy patients were easier to identify by serological assays and typically yielded higher responses than PB patients. Unexpectedly, close examination of patients with a low BI from the Philippines indicated that some patients exhibited strong responses against the ML1556c protein. The responses of Filipino PB patients to ML1556c were often greater than those of MB patients. These results suggested the utility of this protein either as an adjunct to antigens that could identify MB patients to provide a cross-spectrum leprosy diagnosis or as a stand-alone protein for PB leprosy diagnosis. An objective and differential diagnosis of MB or PB leprosy could lead to better treatment of patients by guiding the multidrug therapy regimen provided to them.

We also analyzed the diagnostic potential of each antigen within geographically disparate groups of patients, from the Philippines and two sites in Brazil. In the Brazilian (Goiânia) PB leprosy patient group, ML1556c provided only a few positive responses; this dampened the enthusiasm for ML1556c to be a widely used diagnostic or prognostic leprosy antigen. Of interest, many PB leprosy patients in Brazil (both Goiânia and Salvador) could be diagnosed by ML0405 reactivity, and several PB patients (Salvador) could be diagnosed with ML2331 reactivity. It is unclear if the differences in the responses of patients from different geographic locations are related to differences in *M. leprae* strains or to regional variations in host genetics. These possibilities might be addressed by analysis of patient sera on fragments of ML1556c or by a survey of anti-ML1556c antibody on lysates of different *M. leprae* strains. Regardless, the observed differences indicate the importance of examining antigen-specific responses in several regions when considering their ability to diagnose leprosy globally.

Given that the ML0405Tr and ML2331 proteins could provide diagnosis of leprosy, we made a fusion protein (LID-1) of these individual components. After ensuring the fusion protein retained reactivity against leprosy sera from Salvador, Brazil, we tested the antigens against sera from Japan. As with results obtained using sera from Brazil, Japanese MB leprosy patient sera reacted as strongly with the fusion LID-1 as with the ML0405 and ML2331 components. In addition, some Japanese PB leprosy patient serum antibodies recognized these antigens.

Studies have argued that the presence of anti-PGL-I antibodies is an indicator of leprosy development, but this has been debated (5, 6, 14, 15). Many contacts of leprosy patients have anti-PGL-I antibodies but do not develop disease, limiting the capacity of PGL-I-based assays to predict disease develop-

ment. Indeed, PGL-I-based tests are typically marketed as a support reagent to confirm clinical diagnosis and aid leprosy classification but are not recommended for use as a stand-alone for diagnosis (19). The differential in responses of sera from contacts that developed leprosy compared with contacts that did not develop leprosy was much greater for LID-1 than PGL-1. We demonstrated that LID-1 is capable of providing an early serological diagnosis of MB leprosy. A clear and early diagnosis was achieved in 7 of 11 contacts of leprosy patients who themselves went on to develop clinical leprosy. For the small panel of sera tested, the time benefit of a LID-1-based diagnosis over a clinical-based diagnosis was 6 to 8 months. Thus, screening for LID-1-reactive antibodies, either in the general population or within more focused at-risk populations, could significantly expedite treatment of leprosy patients and, also, affect transmission rates by reducing the number of individuals who develop large bacterial burdens. As another benefit, antibody levels against LID-1 dropped following the implementation of drug treatment in these individuals, and thus the reduction and disappearance of antibodies against LID-1 may be a useful measure of multidrug therapy efficacy.

We are currently evaluating additional antigens, diagnostic formats, and different geographic sources of patient sera with the objective of early and simple identification of leprosy patients regardless of incidence locality.

ACKNOWLEDGMENTS

REFERENCES

1. Anderson, H., B. Stryjewska, B. L. Boyanton, and M. R. Schwartz. 2007. Hansen disease in the United States in the 21st century: a review of the literature. Arch. Pathol. Lab. Med. 131:982–986.
2. Bakker, M. I., M. Hatta, A. Kwenang, P. Van Mosseveld, W. R. Faber, P. R. Klatser, and L. Oskam. 2006. Risk factors for developing leprosy—a population-based cohort study in Indonesia. Lepr. Rev. 77:48–61.
3. Buhrer, S. S., H. L. Smits, G. C. Gussenhoven, C. W. van Ingen, and P. R. Klatser. 1998. A simple dipstick assay for the detection of antibodies to phenolic glycolipid-I of Mycobacterium leprae. Am. J. Trop. Med. Hyg. 58:133–136.
4. Buhrer-Sekula, S., H. L. Smits, G. C. Gussenhoven, J. van Leeuwen, S. Amador, T. Fujiwara, P. R. Klatser, and L. Oskam. 2003. Simple and fast lateral flow test for classification of leprosy patients and identification of contacts with high risk of developing leprosy. J. Clin. Microbiol. 41:1991–1995.
5. Cartel, J. L., S. Chanteau, J. P. Boutin, R. Plichart, P. Richez, J. F. Roux, and J. H. Grosset. 1990. Assessment of anti-phenolic glycolipid-I IgM levels using an ELISA for detection of M. leprae infection in populations of the South Pacific Islands. Int. J. Lepr. Other Mycobact. Dis. 58:512–517.
6. Chanteau, S., P. Glaziou, C. Plichart, P. Luquiaud, R. Plichart, J. F. Faucher, and J. L. Cartel. 1993. Low predictive value of PGL-I serology for the early diagnosis of leprosy in family contacts: results of a 10-year prospective field study in French Polynesia. Int. J. Lepr. Other Mycobact. Dis. 61:533–541.
7. Cho, S. N., R. V. Cellona, L. G. Villahermosa, T. T. Fajardo, Jr., M. V. Balagon, R. M. Abalos, E. V. Tan, G. P. Walsh, J. D. Kim, and P. J. Brennan. 2001. Detection of phenolic glycolipid I of Mycobacterium leprae in sera from leprosy patients before and after start of multidrug therapy. Clin. Diagn. Lab. Immunol. 8:138–142.
8. Cho, S. N., D. L. Yanagihara, S. W. Hunter, R. H. Gelber, and P. J. Brennan. 1983. Serological specificity of phenolic glycolipid I from Mycobacterium leprae and use in serodiagnosis of leprosy. Infect. Immun. 41:1077–1083.
9. Costa, M. B., P. F. Cavalcanti Neto, C. M. Martelli, M. M. Stefani, J. P. Maceira, M. K. Gomes, A. P. Schettini, P. F. Rebello, P. E. Pignataro, E. S.

Ueda, K. Narahashi, and D. M. Scollard. 2001. Distinct histopathological patterns in single lesion leprosy patients treated with single dose therapy (ROM) in the Brazilian Multicentric Study. Int. J. Lepr. Other Mycobact. Dis. 69:177–186.

10. Deps, P. D., B. V. Guedes, J. Bucker Filho, M. K. Andreatta, R. S. Marcari, and L. C. Rodrigues. 2006. Characteristics of known leprosy contact in a high endemic area in Brazil. Lepr. Rev. 77:34–40.

11. Douglas, J. T., R. V. Cellona, T. T. Fajardo, Jr., R. M. Abalos, M. V. Balagon, and P. R. Klatser. 2004. Prospective study of serological conversion as a risk factor for development of leprosy among household contacts. Clin. Diagn. Lab. Immunol. 11:897–900.

12. Fine, P. E., J. A. Sterne, J. M. Ponnighaus, L. Bliss, J. Saui, A. Chihana, M. Munthali, and D. K. Warndorff. 1997. Household and dwelling contact as risk factors for leprosy in northern Malawi. Am. J. Epidemiol. 146:91–102.

13. Flower, C., D. Gaskin, and S. Marquez. 2007. A case of recurrent rash and leg numbness mimicking systemic rheumatic disease: the occurrence of leprosy in a nonendemic area. J. Clin. Rheumatol. 13:143–145.

14. Gonzalez-Abreu, E., J. A. Pon, P. Hernadez, J. Rodriguez, E. Mendoza, M. Hernandez, E. Cuevas, and A. B. Gonzalez. 1996. Serological reactivity to a synthetic analog of phenolic glycolipid I and early detection of leprosy in an area of low endemicity. Lepr. Rev. 67:4–12.

15. Hussain, R., S. Jamil, A. Kifayet, F. Firdausi, H. M. Dockrell, S. Lucas, and R. Hasan. 1990. Quantitation of IgM antibodies to the M. leprae synthetic disaccharide can predict early bacterial multiplication in leprosy. Int. J. Lepr. Other Mycobact. Dis. 58:491–502.

16. Lockwood, D. N., and A. J. Reid. 2001. The diagnosis of leprosy is delayed in the United Kingdom. QJM 94:207–212.

17. Lockwood, D. N., and S. Suneetha. 2005. Leprosy: too complex a disease for a simple elimination paradigm. Bull. W. H. O. 83:230–235.

18. Meima, A., J. H. Richardus, and J. D. Habbema. 2004. Trends in leprosy case detection worldwide since 1985. Lepr. Rev. 75:19–33.

19. Oskam, L., E. Slim, and S. Buhrer-Sekula. 2003. Serology: recent developments, strengths, limitations and prospects: a state of the art overview. Lepr. Rev. 74:196–205.

20. Reece, S. T., G. Ireton, R. Mohamath, J. Guderian, W. Goto, R. Gelber, N. Groathouse, J. Spencer, P. Brennan, and S. G. Reed. 2006. ML0405 and ML2331 are antigens of Mycobacterium leprae with potential for diagnosis of leprosy. Clin. Vaccine Immunol. 13:333–340.

21. Ridley, D. S., and W. H. Jopling. 1966. Classification of leprosy according to immunity. A five-group system. Int. J. Lepr. Other Mycobact. Dis. 34:255–273.

22. Roche, P. W., W. J. Britton, S. S. Failbus, D. Williams, H. M. Pradhan, and W. J. Theuvenet. 1990. Operational value of serological measurements in multibacillary leprosy patients: clinical and bacteriological correlates of antibody responses. Int. J. Lepr. Other Mycobact. Dis. 58:480–490.

23. Roche, P. W., S. S. Failbus, W. J. Britton, and R. Cole. 1999. Rapid method for diagnosis of leprosy by measurements of antibodies to the M. leprae 35-kDa protein: comparison with PGL-I antibodies detected by ELISA and "dipstick" methods. Int. J. Lepr. Other Mycobact. Dis. 67:279–286.

24. Scollard, D. M. 2004. Classification of leprosy: a full color spectrum, or black and white? Int. J. Lepr. Other Mycobact. Dis. 72:166–168.

25. Van Buynder, P., J. Eccleston, J. Leese, and D. N. Lockwood. 1999. Leprosy in England and Wales. Commun. Dis. Public Health 2:119–121.

26. WHO. 2005. Global leprosy situation, 2005. Wkly. Epidemiol. Rec. 80:289–295.

27. WHO. 2007. Global leprosy situation, 2007. Wkly. Epidemiol. Rec. 82:225–232.

28. Young, D. B., and T. M. Buchanan. 1983. A serological test for leprosy with a glycolipid specific for Mycobacterium leprae. Science 221:1057–1059.

Mycobacterium tuberculosis Infects Dendritic Cells with High Frequency and Impairs Their Function In Vivo[1]

Andrea J. Wolf,[*†] Beth Linas,[*] Giraldina J. Trevejo-Nuñez,[*] Eleanor Kincaid,[*†]
Toshiki Tamura,[‡] Kiyoshi Takatsu,[2§] and Joel D. Ernst[2*†¶‖]

Mycobacterium tuberculosis (Mtb) is thought to reside in macrophages, although infected dendritic cells (DCs) have been observed. Thus, although cellular associations have been made, global characterization of the cells harboring Mtb is lacking. We have performed temporal and quantitative characterization of the cells harboring Mtb following aerosol infection of mice by using GFP-expressing bacteria and flow cytometry. We discovered that Mtb infects phagocytic cells of diverse phenotypes, that the predominant infected cell populations change with time, and that myeloid DCs are the major cell population infected with Mtb in the lungs and lymph nodes. We also found that the bacteria in the lung-draining lymph node are transported there from the lungs by a CCL19/21-dependent mechanism and that the transport of bacteria to the lymph node is a transient phenomenon despite chronic infection. In addition, we found that the lymph node cell subsets that are most efficacious in stimulating Mtb-specific, TCR-transgenic CD4^{+} T lymphocytes are not infected with the bacteria and are scarce or absent from the lungs of infected mice. Finally, we found that the lung cell populations that are infected with Mtb at high frequency are relatively ineffective at stimulating Ag-specific CD4^{+} T lymphocytes, and we have obtained evidence that live Mtb can inhibit MHC class II Ag presentation without a decrease in the surface expression of MHC class II. These results indicate that Mtb targets DC migration and Ag presentation in vivo to promote persistent infection. *The Journal of Immunology*, 2007, 179: 2509–2519.

*M*ycobacterium tuberculosis (Mtb)[3] is an exceptionally successful pathogen, which indicates that it is particularly successful at evading immune responses. Humans and experimental animals infected with Mtb exhibit robust Ag-specific CD4^{+} Th1 and CD8^{+} T lymphocyte responses to Mtb Ags (1–3), implying that the initial steps in the priming and differentiation of T lymphocytes are functional in the setting of tuberculosis. However, since the early 20th century it has been known that Mtb is rarely, if ever, eliminated after infection (4–6).

A major challenge to developing more efficacious vaccines against tuberculosis is the incomplete understanding of the mech-

anism of immunity and the mechanism of immune evasion by Mtb. Despite strong evidence that in humans (7, 8) and mice (1) CD4^{+} T lymphocytes with a Th1 phenotype (9, 10) are essential for preventing rapid progression of Mtb disease, little is known regarding the cellular mechanisms of the initiation of CD4^{+} T cell responses following Mtb infection, and it is unclear how Mtb evades elimination once an adaptive immune response develops.

For >70 years (11) it has been known that Mtb survives within macrophages in the lungs, but it is unlikely that lung macrophages alone are capable of initiating cellular immune responses by activating Ag-specific naive CD4^{+} T lymphocytes. Recently, dendritic cells (DCs) have been found to contain Mtb in human (12) and mouse (13) tissues, and the depletion of CD11c^{+} cells (including DCs) in mice before an i.v. injection of Mtb delays the development of CD4^{+} T cell responses and results in impaired immune control of Mtb (14). Although these data provide evidence that DCs can contain Mtb and that they can contribute to the timely development of protective immunity, the precise roles of DCs and macrophages in the trafficking of bacteria and initiation of immunity and as reservoirs of bacteria in tuberculosis remain undefined. Moreover, it is unclear how each of these cellular subsets interacts with Ag-specific T lymphocytes in lungs and lymph nodes to provide limited protective immunity in tuberculosis.

We developed a technique for sensitive and specific flow cytometry detection and phenotyping of cells from mice infected with GFP-expressing Mtb and found that DCs are infected with Mtb at high frequency in the lungs and draining lymph nodes after aerosol infection. We also found that DCs transport Mtb from the lungs to the local draining lymph node, but the frequency of transport decreases markedly after a peak in the 3rd week of infection. Moreover, we found that the subsets of cells that are infected at high frequency in vivo are poor stimulators of Mtb Ag-specific CD4^{+} T cells despite expressing surface MHC class II and co-stimulatory molecules.

*Division of Infectious Diseases, Department of Medicine, New York University School of Medicine, New York, NY 10016; †Biomedical Sciences Graduate Program, University of California, San Francisco, CA 94143; ‡Department of Microbiology, Leprosy Research Center, National Institute of Infectious Disease, Tokyo, Japan; §Department of Microbiology and Immunology, Division of Immunology, Institute of Medical Science, University of Tokyo, Tokyo, Japan; ¶Department of Pathology and ‖Department of Microbiology, New York University School of Medicine, New York, NY 10016

[2] Address correspondence and reprint requests to Dr. Joel D. Ernst, Division of Infectious Diseases, New York University School of Medicine, Smilow Research Center, Room 901, 550 First Avenue, New York, NY 10016; E-mail address: joel.ernst@med.nyu.edu or Dr. Kiyoshi Takatsu, Department of Microbiology and Immunology, Division of Immunology, Institute of Medical Science, University of Tokyo, 4-6-1 Shirokane-dai, Minato-ku, Tokyo, Japan; E-mail address: takatsuk@ims.u-tokyo.ac.jp

[3] Abbreviations used in this paper: Mtb, *Mycobacterium tuberculosis*; ADC, albumin dextrose catalase; β-gal, β-galactosidase; DC, dendritic cell; Tg, transgenic.

Materials and Methods

Mice

C57BL/6J mice were bred and housed in the New York University School of Medicine (New York, NY) animal facilities or purchased from The Jackson Laboratory. *plt/plt* (backcrossed against C57BL/6 for 10 generations, obtained from S. Luther and J. Cyster, University of California, San Francisco, CA), and P25 TCR-transgenic (Tg) mice were bred and housed in the New York University animal facility. Mice were infected at 8–12 wk of age.

Mtb strains and growth

Mtb (H37Rv) was transformed with the plasmid pMV262 encoding FACS-optimized GFPmut3 under the control of the *Mycobacterium bovis* BCG Hsp60 promoter (provided by Dr. L. Ramakrishnan, University of Washington, Seattle, WA). Bacteria were grown in Middlebrook 7H9 medium supplemented with 10% (v/v) albumin dextrose catalase (ADC) enrichment and 50 μg/ml kanamycin. Aerosol infection stocks were generated by initial passage in C57BL/6J mice. After 36 days of infection, lungs were homogenized and plated on Middlebrook 7H11 selective medium plates (Difco) with 50 μg/ml kanamycin and grown for 2–3 wk at 37°C. Bacterial colonies were scraped into Falcon T75 flasks containing 7H9+ADC enrichment and grown lying flat to mid-log phase growth for ~7 days at 37°C. Bacteria were pelleted at 2000 × g and resuspended in one-tenth of the original growth volume of PBS containing 0.5% Tween 80, aliquoted, and frozen at −80°C. The aerosol stock titer was determined by preparing eight 10-fold serial dilutions of five random vials of stock in triplicate in PBS containing 0.5% Tween 80 and plating on Middlebrook 7H11 plates.

Antibodies

All Abs were purchased from BD Pharmingen unless otherwise stated. Anti-CD11c PerCP (H3L) was a custom conjugate from BD Pharmingen, and other Ab conjugates used were anti-CD11b allophycocyanin-Cy7, anti-Gr-1 allophycocyanin or PE-Cy7, and anti-CD86 allophycocyanin. Purified anti-CD80, anti-CD40, and anti-I-A/I-E were purchased from BD Pharmingen and conjugated to Alexa Fluor 647 by using a mAb conjugation kit from Molecular Probes.

Mouse aerosol infections

Mice were infected by the aerosol route using an inhalation exposure unit from Glas-Col. An aliquot of aerosol infection stock was thawed at room temperature, and the bacterial suspension was forced 10 times through a 25-gauge needle fitted to a 1-ml syringe to disperse clumps of bacteria. The inoculum was prepared by diluting the bacterial stock of a known concentration to a concentration equal to 2 × 10^4 times the intended dose per mouse in sterile water to yield 6 ml of inoculum. Five milliliters of the inoculum was loaded into the inhalation exposure unit nebulizer and the remaining 1 ml was used to confirm the inoculum concentration by serial dilution and plating on 7H11 agar. The following program was used to infect the mice: 900 s of preheating, 2400 s of nebulizing, 2400 s of cloud decay, and 900 s of decontamination. After infection, mice were returned to their original cages and housed in individually ventilated microisolator cages. For controls for the specificity of GFP fluorescence as a measure of infection, a group of C57BL/6J mice were infected with wild-type Mtb H37Rv by the same procedure within 24 h of the Mtb-GFP group. For all infections, the actual infection dose was determined by euthanizing five mice within 24 h of infection. Lungs were removed, homogenized, and plated on 7H11 agar plates. CFU were counted after incubation at 37°C for 2–3 wk.

Tissue harvests and CFU determination

Mice were euthanized by CO_2 followed by cervical dislocation. The lungs and mediastinal lymph nodes were removed and placed in digestion buffer (RPMI 1640, 5% FCS, and 10 mM HEPES). Tissues were minced using forceps and scissors into pieces 2-mm^3 in the greatest dimension. Tissue was then incubated in 1 mg/ml collagenase D (Roche) and 30 μg/ml DNase I (Roche) at 37°C for 45 min. Each tissue was forced through a 70-μm cell strainer (BD Falcon) and an aliquot was removed to determine the bacterial load. The single cell suspension was washed and the RBC were removed using ACK lysis buffer (155 mM NH_3Cl, 10 mM $KHCO_3$, and 88 μM EDTA). Live cells were counted using trypan blue exclusion.

FACS staining and acquisition

Staining for surface markers was done by resuspending 1 × 10^6 cells in medium with an Fc receptor-blocking Ab (clone 2.4G2) for 10 min at 4°C followed by washing and resuspension with FACS buffer (PBS, 1% FCS,

0.1% sodium azide, and 1 mM EDTA) containing Abs and incubation at 4°C for 20 min. Cells were then washed twice and fixed in 1% paraformaldehyde overnight at 4°C. Samples were acquired using a FACSDiva, LSR II, or FACSVantage flow cytometer depending on the experiment. Because Mtb-GFP$^+$ cells are rare, especially early in infection, and lung cells exhibit high autofluorescence, special conditions were required to detect and phenotype Mtb-GFP$^+$ cells. First, unstained lung cells from mice infected with wild-type Mtb H37Rv were used to set the boundary between the GFP$^+$ and negative populations. Second, due to the low frequency of GFP$^+$ cells, an abundant positive control was required to standardize the GFP compensation. For this purpose, RAW264.7 cells were transformed with the plasmid pEGFP-N1 (Clontech Laboratories) and a stable GFP-expressing line (RAW-GFP) was generated. RAW-GFP cells were spiked into a sample of unstained lung cells to compensate the GFP. Finally, because of the autofluorescence associated with lung cells it was not possible to use Abs conjugated to fluorophores spectrally adjacent to GFP. An empty/unused channel was necessary to establish a consistent GFP$^+$ gate. Mtb-GFP$^+$ cells could then be phenotyped using fluorophores with at least one spectral channel of distance from GFP.

Phenotyping and quantitation of lung and lymph node cells

CD11c^{high}CD11b^{high} lung cells were designated as myeloid DCs based on previously described functional and morphologic characteristics (15–17) and on the observation that, after aerosol infection of IFN-γR$^{-/-}$ mice with Mtb, they expressed high levels of surface MHC class II whereas in other lung cell subsets surface class II expression was markedly reduced in infected IFN-γR$^{-/-}$ mice (data not shown). Alveolar macrophages (CD11c^{high}CD11b^{low}) were identified by the pattern of staining of cells recovered by bronchoalveolar lavage and by the depletion of this cell subset from postlavage lung homogenates. Recruited macrophages (CD11c^{low}CD11b^{high}) were identified by their presence in low numbers in uninfected mice, their absence from bronchoalveolar lavage, the marked increase in their numbers in the lungs after aerosol infection with Mtb, and their dependence on IFN-γ responsiveness for the surface expression of MHC class II. Monocytes (CD11c$^-$CD11b^{low}) were also identified as in Ref. 15 and expressed low amounts of surface MHC class II in the presence or absence of IFN-γ responsiveness. Neutrophils were identified as described in *Results* on the basis of their nuclear morphology and the presence of myeloperoxidase. Myeloid DCs (CD11c^{high}CD11b^{high}) in mediastinal lymph nodes were identified as described (15, 16). CD11c$^+$CD11b^{low} lymph node cells, despite their resemblance in terms of expression of these markers, were considered to be distinct from alveolar macrophages in the lung because they are present in lymph nodes that do not drain the lungs. They and the CD11c$^+$CD11b$^-$ cells are likely to be similar, if not identical, to DC subsets previously identified in mouse lymph nodes (18, 19).

Mtb expressing β-galactosidase (β-gal) and immunohistochemistry

Mtb H37Rv was transformed with the plasmid pUS989 (a gift from Dr. D. McIntosh, Oswaldo Cruz Foundation, Rio de Janeiro, Brazil), which expresses β-galactosidase under the control of the Hsp60 promoter (20), to prepare a strain termed Mtb-β-gal. Wild-type C57BL/6 mice were infected with mouse-passaged Mtb-β-gal by the aerosol route as described above. At designated time points lungs were inflated with Tissue-Tek OCT (Sakura Finetek) and embedded and frozen in Tissue-Tek OCT. Samples were stored at −80°C. Tissue was sectioned into 6-μm sections using a Leica cryostat fitted with a CryoJane tape-transfer system and a Cryo-Vac-Away system (Instrumedics). Sections were dried and fixed for 10 min with acetone. Mtb-β-gal was detected in sections by staining with a solution of 1 mM $MgCl_2$, 5 mM potassium ferrocyanide, 5 mM potassium ferricyanide, and 1 mg/ml X-galactosidase in PBS for 12 h at 37°C. Immunohistochemistry was performed using a mAb to DEC-205 (NLDC-145; Serotec), which was detected using biotin-labeled anti-rat IgG (Vector Laboratories) and a Vector ABC alkaline phosphatase kit using Vector Red as the substrate (Vector Laboratories). Sections were counterstained with Vector hematoxylin and mounted using Permount. Sections were viewed and photographed using a Leica DMRB microscope using a ×20 or a ×100 oil objective and equipped with a Diagnostics Instruments Spot Slider camera and Spot software.

Cell sorting and microscopy

Paraformaldehyde-fixed, single-cell suspensions of lung and lymph nodes were stained with 4′,6′-diamidino-2-phenylindole (Molecular Probes) and ~1000 cells were sorted onto slides based on CD11b and CD11c surface stains using a FACS Vantage (New York University Center for AIDS Research, New York NY). Cells were mounted using Slow-Fade mounting